A Two-stage Stochastic Programming Approach for CRNA Scheduling with Handovers

Abhishrut Sinha
Department of Systems Science and Industrial Engineering, State University of New York, Binghamton

Ankit Bansal
Department of Systems Science and Industrial Engineering, State University of New York, Binghamton

Osman Ozaltin
Edward P. Fitts Department of Industrial and Systems Engineering, North Carolina State University

Michael Russell
Department of Anesthesiology, West Virginia University School of Medicine

We present a two-stage stochastic integer program for assigning Certified Registered Nurse Anesthetists (CRNAs) to Operating Rooms (ORs) under surgery duration uncertainty. The proposed model captures the trade-offs between CRNA staffing levels, CRNA handovers and under-staffing in the ORs. Since the stochastic program includes binary variables in both stages, we present an Integer L-shaped Algorithm to solve the model that incorporates LP Benders Cuts in addition to the standard *no-good* cuts. To further accelerate convergence, we strengthen these LP Benders Cuts by tightening the second-stage formulation. To this end, we derive valid inequalities for the second-stage problem and show that they describe the convex hull of a binary set defined by a subset of the second-stage constraints. An extensive computational study, based on the data from our partner institution, reveals that our proposed solution approach efficiently solves realistic problem instances to 0.01-optimality, underscoring the effectiveness of the proposed valid inequalities. Additionally, through sensitivity analysis, we provide insights into the trade-offs between CRNA staffing levels, CRNA handovers and under-staffing.

Key words: CRNA Scheduling, Handovers, Two-Stage Stochastic Integer Program, Integer L-shaped Algorithm, Valid Inequalities

History:

1. Introduction

Medical errors are detrimental to patients' health and cost healthcare providers millions of dollars in punitive charges and litigation. A significant portion of these errors stems from communication failures (Kazemian et al. 2014). Transfer of care from one provider to another, also known as handovers, is a major source of such failures and lower clinical quality, as critical details can be lost in the transition (Boet et al. 2020, Saager et al. 2014).

In this paper, we focus on intraoperative handovers between Certified Registered Nurse Anesthetists (CRNAs) that involve transferring the responsibility for a patient's anesthesia care from one provider to another during a surgery.

A handover between CRNAs occurs because of shift changes or scheduling constraints. This process involves communicating vital information about the patient's status, anesthetic plan, medications administered, airway management, fluid balance, surgical progress, and any intraoperative events or complications that may arise. Ideally, this exchange should be structured and comprehensive to ensure continuity of care. However, handovers frequently occur under time pressure and in noisy, high-stress environments like the operating rooms (ORs), increasing the risk of incomplete or inaccurate communication. Even small omissions, such as neglecting to mention an allergy or a drug dosage, can lead to serious patient harm, including adverse drug reactions or delayed recognition of complications.

Although intraoperative CRNA handovers may be unavoidable for long surgeries due to shift length limits, they should be avoided whenever possible to reduce the likelihood of communication breakdowns and maintain the continuity of care. This can be achieved, for example, if CRNAs work overtime. However, as daily shifts of CRNAs usually exceed 8 hours, working overtime may increase fatigue and lack of concentration, which can eventually increase the risk of medical errors (Bae 2021, Bae and Fabry 2014). In practice, overtime hours of CRNAs are limited by regulatory guidelines or union rules (Bae and Yoon 2014, Mobasher et al. 2011). Scheduling CRNAs on overlapping shifts with different start and end times might be another strategy for reducing handovers and under-staffing in the ORs. We address this decision problem through novel modeling and methodological approaches.

We propose a two-stage stochastic integer program (SIP) for assigning CRNAs to ORs, and demonstrate its application using data from a tertiary medical center in the eastern United States. The proposed model, referred to as Stochastic CRNA Scheduling with Handovers (SCSH), captures the trade-offs between staffing and handovers while accounting for uncertainty in surgery durations. Specifically, given the daily surgery schedules in ORs, the first-stage decisions determine the number of CRNAs to be called for a set of (overlapping) shifts with different start and end times. In the second stage, CRNAs are assigned to ORs over the time periods in their shifts. The objective function minimizes the total cost of CRNA staffing along with the expected costs associated with CRNA handovers and understaffing. The majority of existing nurse scheduling models in the literature focus on using

overtime to mitigate workload uncertainty without accounting for handovers. A limited set of studies that consider handovers typically do so in deterministic settings or assume that handovers have no impact on the quality of care. Our model explicitly minimizes handovers in ORs under uncertain surgery durations, and can be easily extended to consider overtime.

SCSH includes binary variables in both stages, and can be optimized using the Integer L-shaped Algorithm (Laporte and Louveaux 1993). The feasibility and optimality cuts generated in the Integer L-shaped Algorithm tend to be weak, resulting in slow convergence. Therefore, they are usually augmented with LP Benders Cuts (Angulo et al. 2016). The performance of the Integer L-shaped Algorithm can be further improved by tightening the formulation of the second-stage problem.

We derive a set of valid inequalities for the second stage of SCSH. These inequalities define the convex hull of the nurse assignment and handover constraints. Our computational results show that they substantially accelerate the convergence of the Integer L-shaped Algorithm. The proposed valid inequalities are broadly applicable to re-scheduling problems that explicitly consider service (or job) transfers between servers due to limited resource availability or failures. Such problems arise in the preemptive variant of the resource-constrained scheduling problem where activities are interrupted and executed on a different resource when they are at risk of becoming tardy (Kirti et al. 2024), or resumed later to improve the makespan of a project to which they belong (Salvadori and Agnetis 2025, Buddhakulsomsiri and Kim 2006). The proposed valid inequalities can also strengthen the formulations used to design routing-based reactive scheduling policies for machine failures in job shops, where affected jobs are rerouted to alternative machines when their primary machines fail (Kutanoglu and Sabuncuoglu 2001, Zhang et al. 2021). None of these studies in the literature proposed valid inequalities.

The remainder of the paper is organized as follows. Section 2 provides a review of the relevant literature. Section 3 introduces the formulation of SCSH, and Section 4 outlines our solution methodology. Section 5 details the proposed valid inequalities. Section 6 presents the computational experiments and managerial insights. Section 7 concludes the paper.

2. Literature Review

This paper involves both modeling and methodological advancements. Section 2.1 reviews the literature on nurse scheduling and handover processes, while Section 2.2 examines existing approaches for solving two-stage SIPs. Finally, Section 2.3 summarizes our main contributions.

2.1. Nurse Scheduling and Handovers

The literature on nurse scheduling in ORs can generally be divided into two main categories; studies that integrate nurse scheduling with surgery scheduling (Breuer et al. 2020, Guo et al. 2016, Latorre-Núñez et al. 2016, Xiang et al. 2015) and those that concentrate exclusively on nurse scheduling for a given surgery schedule (Di Martinelly and Meskens 2017, Lim et al. 2016, Guo et al. 2014, Mobasher et al. 2011). Among these, some consider the uncertainty in surgery durations (Breuer et al. 2020, Guo et al. 2014, Latorre-Núñez et al. 2016) while others solve a deterministic problem. Additionally, Rath et al. (2017) and Tsang et al. (2025) present models that integrate surgery and anesthesiologist scheduling under surgery duration uncertainty. These papers do not consider handovers between providers and those that consider uncertainty in surgery durations allow providers to work overtime to mitigate the impact of uncertainty. We focus on the allocation of CRNAs to ORs for a given surgery-to-OR allocations and start times. We take into account uncertainty in surgery durations and consider handovers at the end of CRNA shifts instead of overtime. However, the proposed model can be easily adapted to consider overtime.

The existing literature on handovers in scheduling problems within healthcare delivery systems is limited. Kazemian et al. (2014) propose an integer programming approach for designing work shift schedules of medical trainees with the objective of minimizing patient handovers while Smalley et al. (2015) present a mixed-integer programming model for physician scheduling that seeks to reduce patient handovers between physicians. However, both of these papers address deterministic problems in non-surgical settings. Sun et al. (2023) tackle a medium-term, tactical-level anesthesiologist scheduling problem spanning multiple weeks. They develop optimization models for designing shifts and assigning anesthesiologists to these shifts while accounting for uncertainties in clinical demand. In contrast, we address the operational level CRNA scheduling problem for a given set of shifts. In their models, Sun et al. (2023) permit handovers between anesthesiologists but assumes that such transitions do not affect the quality of care. Consequently, unlike our paper, their approach does not aim to reduce or control the number of handovers.

2.2. Solution Methods for Two-Stage SIPs

A substantial body of research exists on solving two-stage SIPs with integer variables in both stages (Küçükyavuz and Sen 2017). The existing literature can be broadly categorized into two main groups. The first group focuses on extending the L-shaped Algorithm

to solve SIPs with integer second-stage variables. This is typically achieved by convexifying the second-stage problem through the addition of valid inequalities, either iteratively (Gade et al. 2014, Zhang and Kucukyavuz 2014, Sen and Higle 2005) or in a single step (Bansal et al. 2018, Kim and Mehrotra 2015). These methods enable the use of L-shaped Algorithm for solving such problems, though the convexification process may be computationally intensive and challenging. The second category addresses SIPs with binary first-stage variables using the Integer L-shaped Algorithm (Laporte and Louveaux 1993, Angulo et al. 2016). This approach follows a Benders-style decomposition framework, where no-good type feasibility and optimality cuts are iteratively added to the Master Problem. In this paper, we integrate the strengths of both approaches. Specifically, we propose an Integer L-shaped Algorithm for SCSH that, in addition to the traditional no-good cuts, incorporates stronger LP Benders Cuts derived from a tighter second-stage formulation.

2.3. Contributions

The main contributions of this paper are as follows:

i. We formulate SCSH, a two-stage SIP, for assigning CRNAs to ORs across overlapping shifts. The proposed model captures the trade-offs between CRNA staffing and handover costs under uncertainty in surgery durations. It is broadly applicable to shift-based multi-period scheduling environments in which handovers and under-staffing arise, conditions that are common across many medical institutions and in several other industries. Additionally, the proposed formulation can be readily extended to incorporate overtime.

ii. We tighten the formulation of the second-stage problem in SCSH by a set of valid inequalities. We demonstrate that the proposed valid inequalities define the convex hull of the nurse assignment and handover constraints. These inequalities have a general scope and can be applied to multi-period scheduling problems that involve the preemptive or reactive transfer of tasks (jobs) across resources.

iii. We present an Integer L-shaped Algorithm for SCSH, in which we augment the traditional no-good cuts with stronger LP Benders Cuts derived from the second-stage problem after incorporating the proposed valid inequalities. Our computational experiments show that these strengthened LP Benders Cuts substantially improve the convergence of the Integer L-shaped Algorithm.

iv. We demonstrate the applicability of SCSH using historical data from a large tertiary care hospital in the eastern United States. The computational results indicate that SCSH

can support anesthesiology departments in determining appropriate CRNA staffing levels by balancing trade-offs among staffing costs, handovers, and under-staffing, while accounting for uncertainty in surgery durations. When handover costs are relatively low compared to staffing costs, the optimal solution recommends calling more CRNAs with shorter shifts, which are then assigned to ORs in a manner that results in more handovers but fewer under-staffed periods. In contrast, when handover costs are relatively high, the model recommends calling more CRNAs with longer shifts, resulting in fewer handovers but more under-staffed periods.

3. Model Formulation

Each CRNA works on a single shift, and there are multiple shifts with different start and end times. These shifts may overlap in the time periods they cover. The first-stage problem selects CRNAs to be called for each shift. This decision can be made in advance of the surgery day as soon as the surgery schedule becomes available. The second-stage problem assigns CRNAs to ORs over time periods in their shifts under different scenarios of surgery time realizations. The objective of our model is to minimize the total cost of CRNA staffing and the expected total cost of handovers and under-staffing.

Let S be the set of shifts, J the set of ORs, and T the set of time periods. Furthermore, let I be the set of CRNAs and $i_d \notin I$ be the index for a "dummy" or float CRNA, which is assigned to an OR when a regular CRNA is not available, representing under-staffing. Let $I_s \subseteq I$ denote the set of CRNAs working shift s, satisfying $I_{s_1} \cap I_{s_2} = \emptyset$ for all $s_1 \neq s_2 \in S$ and $\cup_{s \in S} I_s = I$. Let z_{st} be a binary parameter which equals 1 if shift s covers period t, and 0 otherwise. Let c_s^f denote the cost of a CRNA on shift s, c^h the cost of a handover, and c^i the per-period cost of CRNA under-staffing in an OR.

Let Ω be a finite set of scenarios representing the uncertainty in surgery durations, and p_ω the probability of scenario $\omega \in \Omega$. Binary parameter $\alpha_{jt}(\omega)$ equals 1 if there is an active surgery in OR j in time period t under scenario ω and 0, otherwise. Lastly, let $J_t(\omega) \subseteq J$ be the subset of ORs with an ongoing active surgery in periods t and $t+1$ under scenario ω.

The first-stage binary variable r_i takes the value 1 if CRNA i is called for duty and 0 otherwise. The second-stage binary variable $x_{ijt}(\omega)$ equals 1 if CRNA i is assigned to OR j in time period t under scenario ω, and 0 otherwise. If $x_{i_d jt}(\omega) = 1$, then CRNA under-staffing occurs in OR j during time period t. The binary variable $w_{it}(\omega)$ is equal to 1 if there is a

Table 1 Description of Notations

Sets and Parameters	
I	set of CRNAs
I_s	set of CRNAs working shift s
J	set of ORs
T	set of time periods
S	set of CRNA shifts
Ω	set of all scenarios
c_s^f	cost of calling a CRNA for shift s
c^h	cost of a handover
c^i	per-period cost of CRNA under-staffing in an OR
z_{st}	binary parameter equal to 1 if shift s covers period t, 0 otherwise
p_ω	probability of scenario ω
$J_t(\omega)$	subset of ORs with same surgery active in periods t and $t+1$ under scenario ω
$\alpha_{jt}(\omega)$	1 if there is an active surgery in OR j in time period t under scenario ω, 0 otherwise
Indices	
i	index of CRNA, $i \in I$
i_d	index of the dummy CRNA, $i_d \notin I$
j	index of OR, $j \in J$
t	index of time period, $t \in T$
s	index of shift, $s \in S$
ω	index of scenario, $\omega \in \Omega$
First-stage decision variables	
r_i	1 if CRNA i is called for duty, 0 otherwise
Second-stage decision variables	
$x_{ijt}(\omega)$	1 if CRNA i is allocated to OR j in time period t under scenario ω, 0 otherwise
$w_{it}(\omega)$	1 if a handover occurs from regular CRNA i to any other CRNA at the end of time period t under scenario ω, 0 otherwise
$\bar{w}_{it}(\omega)$	1 if a handover occurs from a dummy CRNA to regular CRNA i at the end of time period t under scenario ω, 0 otherwise

handover from CRNA i at the end of time period t under scenario ω, and 0 otherwise. Finally, binary variable $\bar{w}_{it}(\omega)$ is equal to 1 if a handover occurs from dummy CRNA to a regular CRNA i at the end of time period t under scenario ω, and 0 otherwise. Table 1 summarizes the notation. Note that the first-stage variable r_i is defined for each CRNA because capturing handovers in the second stage requires tracking whether the same CRNA is assigned to an OR in periods t and $t+1$. This necessitates assigning individual CRNAs to ORs, and only those CRNAs called for duty in the first-stage are available in the second-stage.

We use boldface lowercase letters to denote vectors and boldface uppercase letters to represent matrices. The two-stage SIP is given by:

$$(\texttt{SCSH}) \quad v^* = \text{Min} \sum_{s\in S}\sum_{i\in I_s} c_s^f r_i + \mathcal{Q}(\mathbf{r}) \tag{1a}$$

$$\text{s.t. } r_{i_1} \geq r_{i_2} \qquad \forall s \in S,\ i_1, i_2 \in I_s :\ i_1 < i_2 \tag{1b}$$

$$\mathbf{r} \in \mathbb{B}^{|I|}. \tag{1c}$$

Constraint (1b) is a symmetry-breaking constraint that ensures CRNAs in each shift are selected in increasing order of their indices. The objective function (1a) minimizes the CRNA staffing cost along with the expected total cost of handovers and under-staffing $\mathcal{Q}(\mathbf{r}) \coloneqq \mathbb{E}_\omega Q(\omega, \mathbf{r}) = \sum_{\omega\in\Omega} p_\omega Q(\omega, \mathbf{r})$, where

$$(SS_{\mathbf{r},\omega}) \;\; Q(\omega,\mathbf{r}) = \text{Min} \;\; \sum_{i\in I}\sum_{t\in T} c^h w_{it}(\omega) + \sum_{i\in I}\sum_{t\in T} c^h \bar{w}_{it}(\omega) + \sum_{j\in J}\sum_{t\in T} c^i x_{i_d jt}(\omega) \tag{2a}$$

$$\text{s.t.} \;\; \sum_{j\in J} x_{ijt}(\omega) \le r_i z_{st} \qquad \forall i \in I_s, s \in S, t \in T, \tag{2b}$$

$$w_{it}(\omega) \ge x_{ijt}(\omega) - x_{ij(t+1)}(\omega) \qquad \forall i \in I, j \in J_t(\omega), t \in T \setminus \{|T|\}, \tag{2c}$$

$$\bar{w}_{it}(\omega) \ge x_{i_d jt}(\omega) + x_{ij(t+1)}(\omega) - 1 \qquad \forall i \in I, j \in J_t(\omega), t \in T \setminus \{|T|\}, \tag{2d}$$

$$x_{i_d jt}(\omega) + \sum_{i\in I} x_{ijt}(\omega) = \alpha_{jt}(\omega) \qquad \forall j \in J, t \in T, \tag{2e}$$

$$\mathbf{x}(\omega) \in \mathbb{B}^{(|I|+1)\times|J|\times|T|}, \;\; \mathbf{w}(\omega), \bar{\mathbf{w}}(\omega) \in \mathbb{B}^{(|I|)\times(|T|-1)}. \tag{2f}$$

Constraint (2b) ensures that each CRNA is assigned to at most one OR in each time period. This constraint also guarantees that CRNAs are assigned to an OR in time period t only if they are scheduled for duty and their shift covers that period, thereby accounting for overlapping CRNA shifts. Constraint (2c) captures handovers from CRNA i at the end of period t. In particular, if CRNA i is assigned to OR $j \in J_t(\omega)$ in period t ($x_{ijt}(\omega) = 1$) but is not assigned to that OR in $t+1$ ($x_{ij,t+1}(\omega) = 0$), then $w_{it}(\omega) = 1$, indicating a handover from CRNA i in period t under scenario ω. There can be at most one handover from CRNA $i \in I$ in a period because (2b) restricts each CRNA i to at most one OR in any period.

Constraint (2c) cannot capture handovers from the dummy CRNA because the dummy CRNA may be assigned to multiple under-staffed ORs in the same period. As a result, applying (2c) to a dummy CRNA would underestimate the number of handovers from the dummy CRNA to regular CRNAs at the end of each time period. Therefore, we capture these handovers through (2d). Specifically, when the dummy CRNA is assigned to OR j in period t ($x_{i_d jt}(\omega) = 1$) under scenario ω and a regular CRNA $i \in I$ is assigned to the same OR j in period $t+1$ ($x_{ij(t+1)}(\omega) = 1$), then a handover occurs from the dummy CRNA to regular CRNA i at the end of time period t, which is recorded by setting $\bar{w}_{it}(\omega) = 1$ in (2d). Moreover, since each regular CRNA $i \in I$ is assigned to at most one OR per time period, $\bar{w}_{it}(\omega)$ can be at most 1.

Constraint (2e) ensures that a CRNA (regular or dummy) is assigned to ORs for every time period with an active surgery. The objective function (2a) minimizes the total cost of handover and CRNA under-staffing. Handovers from the dummy CRNA to a regular CRNA involve transferring care from a *float* CRNA to a regular one; hence, it constitutes an actual exchange in the responsibility of care and is therefore penalized in the objective function. SCSH has complete recourse because calling no CRNAs for duty by setting $r_i = 0,\ i \in I$ in the first stage and assigning the dummy CRNA to all ORs in all time periods in by setting $x_{i_d jt}(\omega) = \alpha_{jt}(\omega)\ \ \forall j \in J,\ t \in T$ in the second-stage is a feasible solution.

The proposed model captures the trade-offs between CRNA staffing and handover costs under uncertainty in surgery durations. It accommodates nurse (worker) shifts and surgery (job) schedules with heterogeneous start and end times, making it broadly applicable to shift-based multi-period scheduling environments in which handovers and under-staffing arise, conditions that are common across many medical institutions and in several other industries. Although we assume each CRNA works on a single shift, that is, $I_{s_1} \cap I_{s_2} = \emptyset$ for all $s_1 \neq s_2 \in S$—as is the case at our partner medical institution—the SCSH can be easily modified to handle situations where a CRNA works multiple shifts. For example, if CRNA $i \in I_{s_1} \cap I_{s_2}$, we can replace i with two distinct indices, i_1 and i_2, where $i_1 \in I_{s_1}$ and $i_2 \in I_{s_2}$, and then add the constraint $r_{i_1} + r_{i_2} \leq 1$ to the first-stage problem to prevent calling CRNA i for two different shifts. Lastly, we can extend SCSH to consider CRNA over time by tracking the last time period in which CRNAs are allocated to an OR after their shift ends, as shown in Appendix D. These extensions will not impact the methodological approaches that we propose for the efficient solution of SCSH.

4. Integer L-shaped Algorithm for SCSH

The L-shaped Algorithm can be applied to solve SCSH after relaxing the integrality of the second-stage binary variables. The algorithm generates LP Benders Cuts whenever an integer first-stage solution is identified within a Branch-and-Bound framework (see Appendix A for more details). The optimal objective value of the relaxed problem provides a lower bound for SCSH. Furthermore, the first-stage solution $\mathbf{r}$ obtained from the L-shaped Algorithm can be used to evaluate $\mathcal{Q}(\mathbf{r})$ and derive an upper bound. However, this approach does not ensure global optimality.

The Integer L-shaped Algorithm (ILS) can be applied to obtain the global optimal solution to SCSH. This method can also be also executed within a Branch-and-Bound framework, where the algorithm is initialized with the following master problem:

$$(\mathcal{M}) \quad \text{Min} \sum_{s\in S}\sum_{i\in I_s} c_s^f r_i + \sum_{\omega\in\Omega} p_\omega \theta_\omega \tag{3a}$$

$$\text{s.t. } r_{i_1} \geq r_{i_2} \qquad \forall s \in S,\ \ i_1, i_2 \in I_s :\ \ i_1 < i_2 \tag{3b}$$

$$\theta_\omega \geq 0 \qquad \forall \omega \in \Omega \tag{3c}$$

$$\mathbf{r} \in \mathbb{B}^{|I|} \tag{3d}$$

where θ_ω is an auxiliary variable representing the second-stage cost under scenario ω. Subsequently, for each integer solution $(\bar{\boldsymbol{\theta}}, \bar{\mathbf{r}})$ encountered during the Branch-and-Bound algorithm, and for every scenario ω where $\bar{\theta}_\omega < Q(\omega, \bar{\mathbf{r}})$, the following Integer Optimality Cut is added to $\mathcal{M}$:

$$\theta_\omega \geq Q(\omega, \bar{\mathbf{r}}) \left(\textstyle\sum_{i\in S(\bar{\mathbf{r}})} r_i - \sum_{i\notin S(\bar{\mathbf{r}})} r_i - |S(\bar{\mathbf{r}})| \right) + Q(\omega, \bar{\mathbf{r}}), \tag{4}$$

where $S(\bar{\mathbf{r}}) = \{i \in I | \bar{r}_i = 1\}$. This cut eliminates the solution $(\bar{\boldsymbol{\theta}}, \bar{\mathbf{r}})$ if $\bar{\theta}_\omega < Q(\omega, \bar{\mathbf{r}})$ for scenario ω. The right-hand side of (4) equals $Q(\omega, \bar{\mathbf{r}})$ at $\mathbf{r} = \bar{\mathbf{r}}$, yielding the tightest possible underestimation of θ_ω at $\bar{\mathbf{r}}$. However, if $\mathbf{r} \neq \bar{\mathbf{r}}$, (4) becomes redundant since its right-hand side takes on a non-positive value. As a result, Integer Optimality Cuts contribute little to strengthening the lower bounds within the Branch-and-Bound algorithm, which in turn slows the convergence of ILS. The performance can potentially be improved by generating LP Benders Cuts in addition to the Integer Optimality Cuts. This approach, referred to as ILS-L, first attempts to eliminate an integer solution using LP Benders Cuts generated based on the LP relaxation of the second-stage problems. If no LP Benders Cuts are found, Integer Optimality Cuts are added to $\mathcal{M}$ as shown in the optimality cut subroutine in Algorithm 1.

We apply ILS-L to solve SCSH. To accelerate the convergence, we derive valid inequalities to tighten the formulation of second-stage problem $SS_{\mathbf{r},\omega}$ and strengthen the LP Benders Cuts. We demonstrate that the proposed valid inequalities characterize the convex hull of the assignment and handover constraints defined for each CRNA $i \in I$, $t \in T \setminus \{|T|\}$ and ORs in the set J_t.

Algorithm 1 Optimality Cut Subroutine

Input: $(\bar{\mathbf{r}}, [\bar{\theta}_\omega]_{\omega\in\Omega})$
for $\omega \in \Omega$ **do**
  Obtain $Q^l(\omega, \bar{\mathbf{r}})$, objective value of the LP relaxation of $SS_{\mathbf{r},\omega}$
  if $Q^l(\omega, \bar{\mathbf{r}}) > \bar{\theta}_\omega$ **then**
    Add `LP Benders Cut` (13) to $\mathcal{M}$. ▷ `Step 1`
  end if
end for
if No `LP Benders Cuts` are added in Step 1 **then**
  $S(\bar{\mathbf{r}}) \leftarrow \{i : \bar{r}_i = 1\}$
  for $\omega \in \Omega$ **do**
    Obtain $Q(\omega, \bar{\mathbf{r}})$
    if $Q(\omega, \bar{\mathbf{r}}) > \bar{\theta}_\omega$ **then**
      Add `Integer Optimality Cut` (4) to $\mathcal{M}$ ▷ `Step 2`
    end if
  end for
end if

5. Valid Inequalities for $SS_{\mathbf{r},\omega}$

In this section, we omit the scenario index ω for clarity of the presentation. For a given first-stage solution $\mathbf{r}$, let $\mathcal{P}(\mathbf{r})$ be the set of feasible second-stage solutions. Proposition 1 presents a set of valid inequalities for $\mathcal{P}(\mathbf{r})$. Proofs of all the propositions are stated in Appendix B.

PROPOSITION 1. *For $i \in I$ and $t \in T \setminus \{|T|\}$, the inequalities*

$$w_{it} \geq \sum_{j\in\bar{J}} \left(x_{ijt} - x_{ij(t+1)}\right) \qquad \forall \bar{J} \subseteq J_t \tag{5}$$

are valid for $\mathcal{P}(\mathbf{r})$.

Valid inequalities in (5) capture a handover from `CRNA` i at the end of time period t if that `CRNA` is assigned to an `OR` in $\bar{J} \subseteq J_t$ during time period t but not assigned an `OR` in the same subset in period $t+1$. The summation over `OR`s on the right-hand side of (5) is valid because `CRNA` i can be assigned to at most one `OR` in $\bar{J}$ in each period t and $t+1$. Thus, the term inside the sum can equal 1 for at most one `OR` in $\bar{J} \subseteq J_t$, and (5) generalizes

(2c) by accounting for handovers within each subset of ORs. Example 1 demonstrates that inequality (5) cut off fractional solutions that are feasible to (2c).

EXAMPLE 1. Consider an instance of $SS_{\mathbf{r},\omega}$ with $I = \{1\}, T = \{1,2\}, r_1 = 1, J = J_1 = \{1,2\}$ and $\alpha_{11} = \alpha_{21} = \alpha_{12} = \alpha_{22} = 1$. The solution $w_{11} = 0.5, \bar{w}_{11} = 0, x_{111} = 0.5, x_{121} = 0.5, x_{112} = 0, x_{122} = 0, x_{i_d 11} = 0.5, x_{i_d 21} = 0.5, x_{i_d 12} = 1, x_{i_d 22} = 1$ is feasible to the LP relaxation of $SS_{\mathbf{r},\omega}$ but violates the following valid inequality (5) for $t = 1$ with $\bar{J} = J_t$:

$$\underbrace{w_{11}}_{0.5} \geq \underbrace{x_{111} + x_{121}}_{1} - \underbrace{x_{112} - x_{122}}_{0}.$$

For $i \in I$, $t \in T \setminus \{|T|\}$, let $\mathcal{Q}_{it}$ be a binary set given by:

$$\mathcal{Q}_{it} = \begin{cases} w_{it} \geq x_{ijt} - x_{ij(t+1)} & \forall j \in J_t, \\ \sum_{j \in J_t} x_{ijt} \leq 1,\ \sum_{j \in J_t} x_{ij(t+1)} \leq 1, & \\ w_{it} \in \{0,1\}, x_{ijt}, x_{ij(t+1)} \in \{0,1\} & \forall j \in J_t \end{cases} \tag{6}$$

Constraints (6) restrict the assignment of CRNA i to at most one OR in J_t during the periods t and $t+1$, and determine whether a handover occurs from CRNA i at the end of period t. This constraint structure commonly appears in multi-period preemptive or reactive scheduling problems, where the transfer of tasks across resources is tracked (Salvadori and Agnetis 2025, Buddhakulsomsiri and Kim 2006).

Let $\tilde{\mathcal{Q}}_{it}$ denote the linear relaxation of $\mathcal{Q}_{it}$. The main theoretical result of this paper pertains to showing that adding valid inequalities (5) to $\tilde{\mathcal{Q}}_{it}$ characterizes the convex hull of $\mathcal{Q}_{it}$, which is denoted by $\text{conv}(\mathcal{Q}_{it})$. The proof is achieved in two steps. First, in Proposition 2, we use a disjunctive programming technique to derive a polyhedron $\mathcal{V}_{it}$ in an extended variable space whose projection onto the space of $(w_{it}, \mathbf{x}_{it}, \mathbf{x}_{i(t+1)})$ variables gives $\text{conv}(\mathcal{Q}_{it})$. Then, in Proposition 3, we utilize *Hoffman's Circulation Theorem* (Hoffman 1976) to show that the $\text{Proj}_{(w_{it}, \mathbf{x}_{it}, \mathbf{x}_{i(t+1)})} \mathcal{V}_{it}$ is characterized by $\tilde{\mathcal{Q}}_{it}$ and inequalities in (5), where the projection operator is defined as $\text{Proj}_{(x)} \mathcal{X} = \{ x : \exists y \text{ such that } (x,y) \in \mathcal{X} \}$.

PROPOSITION 2. *For a given $i \in I$, $t \in T \setminus \{|T|\}$, define the auxiliary variables x^1_{ijt} and $x^1_{ij(t+1)}$ $\forall j \in J_t$. Furthermore, let $\mathcal{V}_{it}$ be the polyhedron given by*

$$x_{ijt} - x_{ij(t+1)} \leq x^1_{ijt} - x^1_{ij(t+1)} \leq w_{it} \qquad \forall j \in J_t, \tag{7a}$$

$$-1 + w_{it} + \sum_{j \in J_t} x_{ijt} \leq \sum_{j \in J_t} x^1_{ijt} \leq w_{it}, \tag{7b}$$

$$-1 + w_{it} + \sum_{j \in J_t} x_{ij(t+1)} \leq \sum_{j \in J_t} x^1_{ij(t+1)} \leq w_{it}, \tag{7c}$$

$$0 \leq x^1_{ijt} \leq x_{ijt} \qquad \forall j \in J_t, \tag{7d}$$

$$0 \leq x^1_{ij(t+1)} \leq x_{ij(t+1)} \qquad \forall j \in J_t. \tag{7e}$$

Then, $\text{conv}(\mathcal{Q}_{it}) = \text{Proj}_{(w_{it}, \mathbf{x}_{it}, \mathbf{x}_{i(t+1)})} \mathcal{V}_{it}$.

Proposition 3 presents the projection of $\mathcal{V}_{it}$ onto $(w_{it}, \mathbf{x}_{it}, \mathbf{x}_{i(t+1)})$ variable space.

PROPOSITION 3. $\text{Proj}_{(w_{it}, \mathbf{x}_{it}, \mathbf{x}_{i(t+1)})} \mathcal{V}_{it}$ *is given by the following set of constraints:*

$$\tilde{\mathcal{Q}}^L_{it} = \begin{cases} (w_{it}, \mathbf{x}_{it}, \mathbf{x}_{i(t+1)}) \in \tilde{\mathcal{Q}}_{it}, \\ w_{it} \geq \sum_{j \in \bar{J}} \left(x_{ijt} - x_{ij(t+1)} \right) \quad \forall \bar{J} \subseteq J_t, |\bar{J}| \geq 2. \end{cases} \tag{8}$$

Using Propositions 2 and 3, we obtain the following corollary, which shows that adding valid inequalities (5) to $\tilde{\mathcal{Q}}_{it}$ yields $\text{conv}(\mathcal{Q}_{it})$.

COROLLARY 1. $\text{conv}(\mathcal{Q}_{it}) = \tilde{\mathcal{Q}}^L_{it}$

Corollary 1 suggests that including valid inequalities (5) to $SS_{\mathbf{r},\omega}$ can lead to a tighter formulation of $SS_{\mathbf{r},\omega}$. Therefore, generating `LP Benders Cuts` based on this formulation can accelerate the convergence of `ILS-L`. For each $i \in I$, $t \in T \setminus |T|$, the number of valid inequalities (5) are exponential in $|J_t|$. The following proposition presents a polynomial size reformulation for these valid inequalities.

PROPOSITION 4. *For* $i \in I$, $t \in T \setminus \{|T|\}$, *valid inequalities* (5) *and* $w_{it} \geq 0$ *can be reformulated as:*

$$w_{it} \geq \sum_{j \in J_t} \beta_{ijt} \tag{9a}$$

$$\beta_{ijt} \geq x_{ijt} - x_{ij(t+1)} \qquad \forall j \in J_t, \tag{9b}$$

$$\beta_{ijt} \geq 0 \qquad \forall j \in J_t. \tag{9c}$$

We implement valid inequalities (5) through (9) in our computational experiments. In the following proposition, we present another family of valid inequalities for $\mathcal{P}(\mathbf{r})$.

PROPOSITION 5. *For each* $i \in I$, $t \in T \setminus \{|T|\}$ *and* $j' \in J$. *The inequality*

$$w_{it} \geq x_{ij'(t+1)} - 1 + \sum_{j \in J_t \setminus j'} x_{ijt} \tag{10}$$

is valid for $\mathcal{P}(\mathbf{r})$.

The valid inequality (10) captures a handover at the end of period t when CRNA i is assigned to OR $j' \in J$ in period $t+1$ and another OR in $J_t \setminus j'$ in period t. Proposition 6 shows that this inequality is weakly dominated by (5). Nonetheless, including both valid inequalities in $SS_{\mathbf{r},\omega}$ provides significant computational benefit as we illustrate in Section 6.1.

PROPOSITION 6. *Valid inequality* (10) *is weakly dominated by* (5).

6. Computational Experiments

Our computational experiments are based on data from a tertiary medical hospital in the eastern United States. The dataset consists of 14,883 surgeries across 24 specialties, spanning a period of 353 working days. For each specialty, Table 10 in Appendix C provides the mean and standard deviation of surgery durations, along with the percentage share of total surgeries attributed to each specialty. We assume that the surgery duration for each specialty follows a log-normal distribution (Neyshabouri and Berg 2017). Table 10 presents the estimated mean and standard deviation of surgery durations. To make the trade-offs between handovers and under-staffing more pronounced and to more precisely evaluate the impact of handovers on staffing decisions, we generate instances with longer surgery durations by scaling the mean and variance of surgery durations by 1.5.

While the parameter z_{st} in $SS_{\mathbf{r},\omega}$ permits CRNA shifts to begin and end any time, following the scheduling practices at our partner institution, surgeries are scheduled to start at 7 a.m. in our computational experiments, and CRNAs work on one of four shifts lasting 8, 10, 12, or 14 hours. We consider a 14-hour planning horizon from 7 a.m. to 9 p.m., divided into $|T|=56$ equal time intervals of 15 minutes each. We experiment with the surgery schedules of three different days. Table 2 reports the total number of surgeries, the total number of ORs, and the number of CRNAs during each of the four shifts across these days. More details about each scheduled surgery, including its specialty, planned start time, and the assigned OR, are provided in Appendix C.

Let c_r denote the hourly cost of a CRNA. Assuming a linear relation, the costs of CRNAs for shifts of 8 hours (c_1^f), 10 hours (c_2^f), 12 hours (c_3^f), and 14 hours (c_4^f) are $8c_r$, $10c_r$, $12c_r$, and $14c_r$, respectively. We use $c_r = 200$ in our experiments. In computational experiments, we simply ensure that (c_s^f) increases with shift length. In practice, the costs of longer shifts may scale non-linearly. The proposed model can readily accommodate such cases.

Table 2 Surgery and Shift Data

	Day 1	Day 2	Day 3
Number of surgeries	56	41	37
Number of open ORs	9	9	9
Number of available CRNAs:			
Shift 1: 7 a.m.- 3 p.m.	3	7	3
Shift 2: 7 a.m.- 5 p.m.	5	6	7
Shift 3: 7 a.m.- 7 p.m.	5	1	3
Shift 4: 7 a.m.- 9 p.m.	2	0	1

While the hourly cost of CRNAs is relatively straightforward to estimate in practice, estimating the costs of under-staffing and handovers is more challenging due to their downstream impacts on clinic operations and patient health outcomes. Consequently, we specify these cost parameters relative to CRNA staffing cost, informed by our medical collaborator's acceptable levels of expected handovers and under-staffing in the resulting schedules. Subsequently, we set handover cost (c_h) and per-period CRNA under-staffing cost (c_i) using the ratios $\psi = \frac{c_h}{c_r}$, and $\chi = \frac{c_i}{c_r}$. We consider three values of $\psi = 30, 40, 50$ and three values of $\chi = 5, 10, 20$. Note that extreme values of these parameters lead to trivial solutions. If ψ or χ is set too high, placing excessive emphasis on avoiding handovers or under-staffing, nearly all CRNAs would be called for duty. Conversely, if these parameters are too low, few or no CRNAs would be scheduled, resulting in a large number of handovers or under-staffed periods. We design a full factorial experiment over the values of ψ and χ, resulting in 9 different *cases* for each $|\Omega|$. Furthermore, we generate three random instances for each of the three days per case, that is, 9 different instances per case.

The remainder of this section is organized as follows: Section 6.1 assesses the strength of the valid inequalities derived in Section 5, while Section 6.2 compares different algorithmic approaches for solving SCSH. Section 6.3 examines the value of incorporating stochasticity in surgery durations, and Section 6.4 provides a sensitivity analysis by varying the handover and under-staffing costs to offer managerial insights.

6.1. Effectiveness of Valid Inequalities

To evaluate the effectiveness of the valid inequalities proposed in Section 5, we solve the extensive formulation of SCSH with a single-scenario, both with and without the valid inequalities. Specifically, for each instance, let $\mathtt{Z}$ represent the optimal objective value when integrality is enforced in both stages of the single-scenario problem. Let $\mathtt{Z}^{\mathtt{I}}$ denote the optimal objective value when the integrality is relaxed in the second-stage. Finally, let $\mathtt{Z}^{\mathtt{I}}_{\mathtt{C}}$ denote the optimal objective value when the second-stage is relaxed, and the valid

Table 3 Average (max) optimality gaps (%) for $\rho_{\{5,10\}}$, $\rho_{\{5\}}$ and $\rho_{\{10\}}$.

Case	ψ—χ	$\rho_{\{5,10\}}$	$\rho_{\{5\}}$	$\rho_{\{10\}}$	IG
1	30—5	100.00 (100.00)	96.62 (100.00)	9.34 (47.55)	11.31 (25.19)
2	30—10	98.52 (100.00)	95.59 (100.00)	5.54 (16.67)	12.56 (20.61)
3	30—20	97.88 (100.00)	96.27 (100.00)	7.69 (25.00)	9.87 (17.18)
4	40—5	100.00 (100.00)	96.30 (100.00)	12.30 (61.54)	9.97 (23.44)
5	40—10	98.18 (100.00)	94.98 (100.00)	4.75 (16.67)	13.95 (24.65)
6	40—20	97.78 (100.00)	95.81 (100.00)	6.82 (21.88)	12.03 (21.28)
7	50—5	100.00 (100.00)	95.24 (100.00)	20.78 (83.52)	8.49 (21.42)
8	50—10	99.61 (100.00)	97.87 (100.00)	6.44 (25.00)	14.05 (27.44)
9	50—20	98.17 (100.00)	96.15 (100.00)	6.16 (18.75)	13.35 (22.26)

inequalities $C \in \{\{(5)\},\{(10)\},\{(5),(10)\}\}$ are included. Although we use the reformulation (9) when implementing (5), for clarity of the exposition, we refer to these valid inequalities using (5). We measure the percentage of the integrality gap ($\mathtt{Z} - \mathtt{Z}^{\mathtt{I}}$) closed by adding the valid inequalities C using $\rho_C = \dfrac{\mathtt{Z}^{\mathtt{I}}_{\mathtt{C}} - \mathtt{Z}^{\mathtt{I}}}{\mathtt{Z} - \mathtt{Z}^{\mathtt{I}}} \times 100$. We set a solution time limit of 3600 seconds using a 14-core Intel Xeon 2.60GHz processor with 128GB RAM, Python 3.9.12 and Gurobi 11.0.2. For each of the 9 cases defined by ψ, χ and for each C, Table 3 reports the average (maximum) ρ_C, and the average (maximum) integrality gap, $\mathtt{IG} = \frac{\mathtt{Z}-\mathtt{Z}^{\mathtt{I}}}{\mathtt{Z}} \times \mathtt{100}$. The table demonstrates that the combination of valid inequalities $\{(5),(10)\}$ closes a substantial portion of integrality gap and, in several instances, fully eliminates it. Moreover, the values of $\rho_{\{5\}}$, and the difference between $\rho_{\{5,10\}}$ and $\rho_{\{5\}}$ indicate that although valid inequalities (5) close a substantial portion of the integrality gap, valid inequalities (10) still provide a significant contribution.

6.2. Computational Performance of Algorithms to Solve SCSH

In this section, we compare the performance of the following five methods to solve SCSH:

1. `L-shaped Algorithm` as detailed in Appendix A with no valid inequalities added to $SS_{\mathbf{r},\omega}$ (`LS-NoVI`).
2. `L-shaped Algorithm` with valid inequalities (5) and (10) added to $SS_{\mathbf{r},\omega}$ (`LS-VI`).
3. `ILS-L` with no valid inequalities added to $SS_{\mathbf{r},\omega}$ (`ILS-L-NoVI`).
4. `ILS-L` with valid inequalities (5) and (10) added to $SS_{\mathbf{r},\omega}$ (`ILS-L-VI`).
5. `Extensive Form` solved using Gurobi 11.0.2 (`ExF`).

For all instances, each method is run with a time limit of 3600 seconds and a target optimality gap of 1%. In the computational results, the execution time of `ILS-L-NoVI` and `ILS-L-VI` may exceed the 3600-second limit on certain instances. This occurs because if the algorithm enters the optimality cut subroutine near the time limit, it is allowed to

Table 4 Average (max) optimality gap (%), $|\Omega|= 500$ scenarios.

Case	ψ — χ	LS-NoVI	LS-VI	ILS-L-NoVI	ILS-L-VI	ExF
1	30—5	10.46 (13.02)	0.88 (1.72)	0.25 (0.84)	0.35 (0.93)	92.94 (95.27)
2	30—10	11.56 (12.52)	0.69 (1.17)	0.32 (0.80)	0.45 (1.00)	92.78 (95.41)
3	30—20	9.28 (10.87)	0.32 (0.61)	0.32 (0.88)	0.40 (0.95)	92.75 (95.65)
4	40—5	9.82 (12.73)	0.91 (1.71)	0.00 (0.00)	0.47 (1.00)	93.92 (96.03)
5	40—10	12.83 (14.09)	0.86 (1.45)	0.52 (3.03)	0.43 (0.99)	93.48 (95.95)
6	40—20	11.42 (13.30)	0.50 (0.91)	1.13 (4.30)	0.53 (1.00)	92.45 (95.95)
7	50—5	8.60 (11.13)	0.91 (1.69)	0.32 (0.94)	0.34 (1.00)	95.22 (101.36)
8	50—10	13.37 (14.89)	0.96 (1.61)	0.11 (1.00)	0.49 (1.00)	92.88 (96.38)
9	50—20	12.83 (14.66)	0.69 (1.24)	0.51 (0.97)	0.53 (1.00)	93.57 (96.21)

finish that subroutine before termination, resulting in the total runtime exceeding 3600 seconds. For each of the 9 cases defined by ψ and χ, Tables 4 and 6 present the average (maximum) % optimality gaps for the five algorithms with $|\Omega|= 500$ and 1000 scenarios, respectively, assuming equal probability for each scenario. Tables 5 and 7 report the corresponding average (maximum) computational times (in seconds) for $|\Omega|= 500, 1000$, respectively. Lastly, Table 8 shows the percentage of instances yielding `0.01-optimal` solutions for $|\Omega|= 500, 1000$.

As shown in these tables, both `LS-VI` and `ILS-L-VI` consistently outperform `LS-NoVI`, `ILS-L-NoVI` and `ExF` across all three performance metrics for both $|\Omega|= 500$ and 1000. This indicates that the inclusion of valid inequalities (5) and (10) substantially strengthens the `LP Benders Cuts` in both the `L-shaped Algorithm` and `ILS-L`, and significantly improves the convergence of the latter. For example, when $|\Omega|= 500$, `ILS-L-VI` obtains `0.01-optimal` solutions for all instances. `ILS-L-NoVI` also reaches `0.01-optimal` solutions for most instances but requires significantly more computational time. Similarly, `LS-VI`—though not an exact method for solving `SCSH`—achieves near-optimal solutions, obtaining `0.01-optimal` solutions for more than half of the instances in most cases, while `LS-NoVI` fails to reach such solutions for any case. A similar trend is observed for $|\Omega|= 1000$ scenarios, with a notable distinction: `ILS-L-NoVI` fails to find `0.01-optimal` solutions for many instances within 3600 seconds, whereas `ILS-L-VI` can still find `0.01-optimal` solutions for the vast majority of the instances. Comparing `LS-VI` and `ILS-L-VI`, we find that both exhibit similar average computational performance due to the impact of valid inequalities (5) and (10). However, unlike `LS-VI`, `ILS-L-VI`—being an exact algorithm for `SCSH`—successfully achieves `0.01-optimal` solutions for nearly all instances.

Table 5 Average (max) run time, $|\Omega|$= 500 scenarios.

Case	ψ — χ	LS-NoVI	LS-VI	ILS-L-NoVI	ILS-L-VI	ExF
1	30—5	550 (764)	850 (1007)	2557 (3384)	1231 (2136)	3602 (3604)
2	30—10	434 (549)	829 (1013)	2071 (2780)	1202 (1884)	3603 (3607)
3	30—20	410 (543)	696 (947)	1827 (2280)	1075 (1997)	3602 (3605)
4	40—5	547 (755)	992 (1174)	2254 (3276)	1130 (2115)	3602 (3604)
5	40—10	454 (569)	905 (1233)	2574 (3665)	1295 (2427)	3602 (3604)
6	40—20	402 (505)	772 (1004)	2499 (3725)	1287 (2463)	3610 (3670)
7	50—5	515 (741)	894 (1174)	1487 (2272)	1277 (2103)	3602 (3605)
8	50—10	454 (556)	895 (1133)	1898 (3194)	1069 (1923)	3602 (3605)
9	50—20	449 (547)	788 (954)	2196 (3549)	1245 (2136)	3602 (3605)

Table 6 Average (max) optimality gap (%), $|\Omega|$= 1000 scenarios.

Case	ψ — χ	LS-NoVI	LS-VI	ILS-L-NoVI	ILS-L-VI	ExF
1	30—5	10.42 (12.89)	0.91 (1.72)	4.19 (7.38)	0.54 (0.97)	93.73 (101.90)
2	30—10	11.58 (12.54)	0.70 (1.10)	4.12 (7.60)	0.64 (1.00)	95.23 (109.79)
3	30—20	9.31 (10.89)	0.31 (0.55)	0.89 (7.44)	1.53 (7.60)	95.93 (107.52)
4	40—5	9.75 (12.65)	0.94 (1.71)	3.54 (9.48)	0.54 (1.00)	93.93 (96.01)
5	40—10	12.81 (14.01)	0.88 (1.38)	7.04 (12.49)	0.51 (1.00)	94.89 (108.52)
6	40—20	11.45 (13.31)	0.50 (0.85)	2.97 (10.04)	0.56 (1.00)	94.94 (111.56)
7	50—5	8.52 (11.14)	0.97 (1.95)	1.48 (4.46)	0.53 (0.94)	94.66 (96.56)
8	50—10	13.32 (14.78)	0.96 (1.55)	7.54 (13.91)	0.46 (1.00)	94.05 (96.36)
9	50—20	12.85 (14.68)	0.70 (1.16)	8.59 (37.91)	0.59 (1.15)	93.57 (96.19)

Table 7 Average (max) run time, $|\Omega|$= 1000 scenarios.

Case	ψ — χ	LS-NoVI	LS-VI	ILS-L-NoVI	ILS-L-VI	ExF
1	30—5	955 (1306)	1628 (1919)	3385 (4180)	2164 (4157)	3606 (3623)
2	30—10	811 (945)	1550 (2059)	3413 (4474)	1966 (2909)	3607 (3618)
3	30—20	734 (962)	1269 (1691)	2513 (3691)	2340 (4613)	3604 (3606)
4	40—5	952 (1369)	1703 (2268)	3216 (4164)	2270 (4056)	3605 (3622)
5	40—10	863 (1052)	1521 (1879)	3344 (3969)	2067 (2847)	3605 (3610)
6	40—20	784 (916)	1370 (1698)	3108 (4469)	2366 (4356)	3606 (3610)
7	50—5	947 (1215)	1645 (2123)	3043 (3755)	2268 (3567)	3603 (3606)
8	50—10	847 (947)	1535 (2150)	3452 (4097)	1850 (3320)	3604 (3609)
9	50—20	844 (1008)	1375 (1745)	3485 (4446)	2915 (5242)	3604 (3610)

Table 8 % of 9 instances yielding `0.01-optimal` solutions in each case.

No. of Scenarios $\|\Omega\|$		500	1000	500	1000	500	1000	500	1000	500	1000
Case	ψ — χ	LS-NoVI		LS-VI		ILS-L-NoVI		ILS-L-VI		ExF	
1	30—5	0	0	67	56	100	33	100	100	0	0
2	30—10	0	0	67	67	100	33	100	100	0	0
3	30—20	0	0	100	100	100	89	100	89	0	0
4	40—5	0	0	33	33	100	44	100	100	0	0
5	40—10	0	0	56	44	89	33	100	100	0	0
6	40—20	0	0	100	100	100	67	100	100	0	0
7	50—5	0	0	33	33	100	67	100	100	0	0
8	50—10	0	0	33	33	78	33	100	100	0	0
9	50—20	0	0	67	67	100	33	100	89	0	0

Table 9 Comparison of `Stochastic Solution` and `Mean Value Solution` ($|\Omega|= 500$).

Case	ψ—χ	VSS	$\kappa_{\texttt{HO}}$	$\kappa_{\texttt{US}}$	$\kappa_{\texttt{SC}}$	$\kappa_{\texttt{S}_1}$	$\kappa_{\texttt{S}_2}$	$\kappa_{\texttt{S}_3}$	$\kappa_{\texttt{S}_4}$
1	30—5	2.71	-12.69	9.58	-2.07	38.89	-34.44	0.00	0.00
2	30—10	4.93	2.84	10.43	-2.33	44.44	-40.00	0.00	0.00
3	30—20	6.26	10.09	8.92	-2.54	55.56	-51.11	0.00	0.00
4	40—5	2.45	-13.85	8.19	-2.33	44.44	-40.00	0.00	0.00
5	40—10	4.76	-2.45	10.66	-2.33	44.44	-40.00	0.00	0.00
6	40—20	6.44	8.63	9.30	-2.54	55.56	-51.11	0.00	0.00
7	50—5	2.36	-7.91	7.06	-2.07	38.89	-34.44	0.00	0.00
8	50—10	4.52	-6.43	10.27	-2.33	44.44	-40.00	0.00	0.00
9	50—20	6.48	5.66	10.75	-4.39	33.33	-40.00	0.00	0.00

6.3. Comparison with the `Mean Value Solution`

To assess the impact of modeling uncertainty in surgery durations, Table 9 compares the best solution obtained from `ILS-L-VI` (`Stochastic Solution`) in Section 6.2 with the `Mean Value Solution` (Birge and Louveaux 2011) for $|\Omega|= 500$. Column 3 of Table 9 reports the average Value of the Stochastic Solution (VSS), computed as $\frac{MV-UB}{MV} \times 100$, where UB and MV denote the objective value evaluated at the `Stochastic Solution` and `Mean Value Solution`, respectively. Columns 4–9 present the average percentage reduction in l when using `Stochastic Solution` relative to `Mean Value Solution`, denoted by $\kappa_l = \frac{l_{MV}-l_{SS}}{l_{MV}}$, where l_{MV} and l_{SS} are the values of l under `Mean Value Solution` and `Stochastic Solution`, respectively. Thus, $\kappa_l > 0$ indicates that the value of l under `Stochastic Solution` is lower than under `Mean Value Solution`, whereas $\kappa_l < 0$ indicates the opposite. In Columns 4 and 5, l corresponds to the expected number of handovers (`HO`) and under-staffing (`US`), respectively. In Column 6, l denotes the first-stage staffing cost (`SC`). Finally, in Columns 7–10, l represents the number of shift k `CRNA`s called for duty ($\texttt{S}_\texttt{k}$) where $\texttt{k} = 1, 2, 3, 4$ (see Table 2). Results for $|\Omega|= 1000$ are presented in Appendix E.

As shown in Column 3 of Table 9, incorporating uncertainty in surgery durations leads to a substantial reduction in the objective value. These savings are primarily driven by lower expected under-staffing and/or handovers under `Stochastic Solution` relative to `Mean Value Solution`, as observed in Columns 4 and 5. This effect arises because, as shown in Columns 6 and 7, `Stochastic Solution` tends to replace Shift 1 `CRNA`s in the `Mean Value Solution` with longer Shift 2 `CRNA`s. This substitution increases coverage and reduces under-staffed periods and/or handovers, and the resulting expected cost savings outweigh the higher staffing costs observed in Column 6. Moreover, this preference for Shift 2 over Shift 1 `CRNA`s becomes more pronounced at higher values of the under-staffing

cost parameter χ, leading to significant reductions in both expected under-staffed periods and handovers. These observations remain consistent when $|\Omega| = 1000$.

6.4. Sensitivity Analysis

In this section, we examine how the expected number of handovers, the expected number of under-staffed time periods, and the number of CRNAs assigned to each shift vary in response to changes in handover cost and under-staffing costs. The results also verify that SCSH captures the trade-offs between staffing cost, handovers, and under-staffing as intended. To better understand these trade-offs, we allow up to 10 CRNAs per shift and consider six values of the handover cost parameter, $\psi \in \{20, 30, 40, 50, 60, 70\}$, along with six values of the per-period under-staffing cost parameter, $\chi \in \{2.5, 5, 10, 20, 30, 40\}$. For these parameter settings, we consider the best solution obtained from LS-VI and ILS-L-VI. Results are averaged over three randomly generated instances of the SCSH corresponding to the Day 3 surgery schedule with $|\Omega| = 500$. As in Section 6.2, LS-VI and ILS-L-VI are solved with a 3600-second time limit, and ILS-L-VI is run with a target optimality gap of 1%.

Figure 1a, for $\chi = 10$, shows the variation in the expected number of handovers and the expected number of under-staffed time periods as the handover cost parameter ψ increases from 20 to 70. Similarly, Figure 1b depicts, for the same value of χ and increasing ψ, the changes in the number of CRNAs assigned per shift and the total cost of CRNAs. Figure 2a and Figure 2b present the same variations for $\psi = 40$ and increasing per-period under-staffing cost parameter χ from 2.5 to 40.

In Figure 1b, the number of CRNAs called for each shift remains the same as ψ increases from 20 to 40. However, we observe in Figure 1a that the average number of handovers decreases while the average number of under-staffed time periods increases as expected. Thus, at a higher handover cost, some surgeries are not assigned any CRNAs because the shifts of all the available CRNAs end during these surgeries, and incurring under-staffing instead of handover is more cost-effective. However, as ψ increases to 50, a Shift 3 CRNA is called in-place of a Shift 2 CRNA. As Shift 3 CRNA can cover a larger number of time periods, both the average number of handovers and the average number of under-staffed time periods decrease at the expense of increased staffing cost.

In Figure 2a, the expected number of handovers increases while the expected number of under-staffed time periods decreases as the per-period under-staffing cost parameter χ increases from 2.5 to 20. This is because both handovers and additional CRNA coverage are

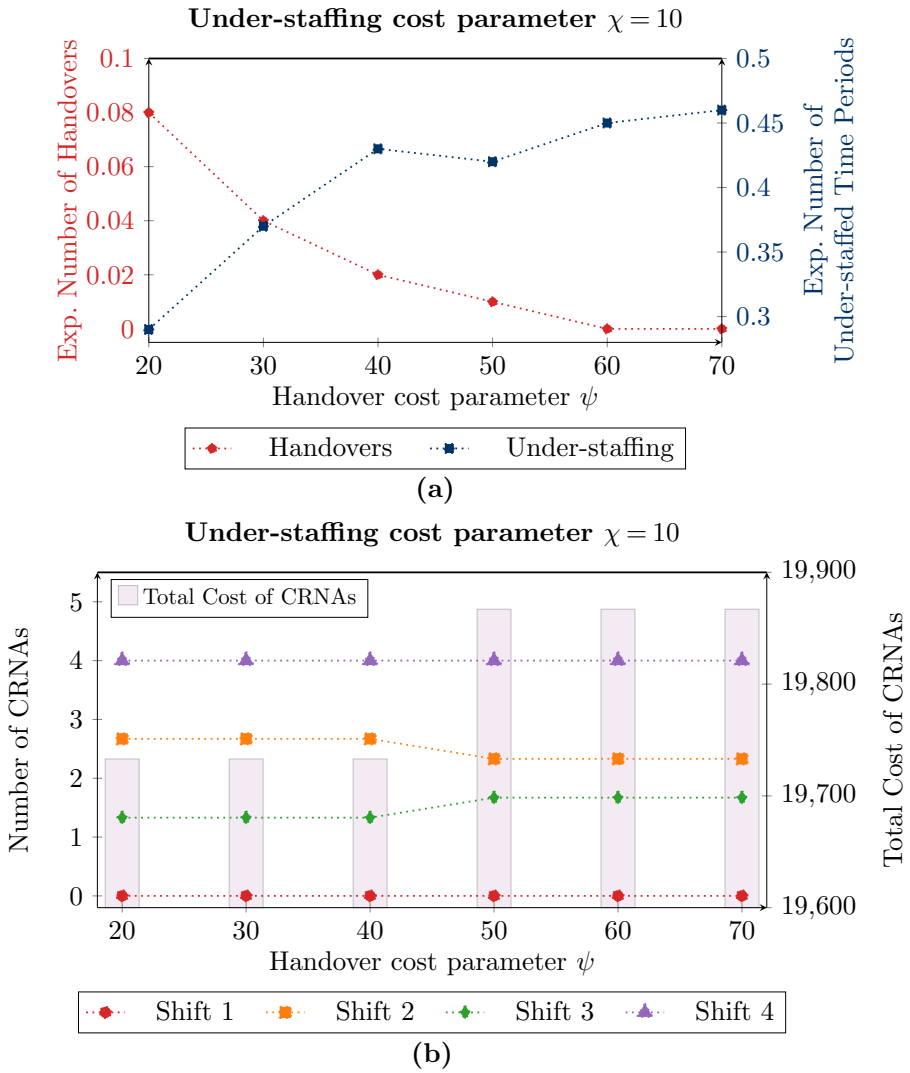

Figure 1 **Analysis of the trade-off between handovers and CRNA staffing.**

used to reduce under-staffing. Additionally, as illustrated in Figure 2b, the total cost of CRNAs increases as χ increases from 2.5 to 20. For example, as χ increases from 5 to 10, Shift 2 and Shift 4 CRNAs are called in-place of Shift 1 and Shift 3 CRNAs. The model favors calling more nurses on longer shifts to cover surgeries scheduled later in the day, where the effects of accumulated duration uncertainty are most pronounced. Lastly, when χ increases to 40, calling an additional Shift 1 CRNA becomes cost-effective, providing sufficient CRNA coverage to reduce both the number of handovers and under-staffed time periods.

7. Conclusion

We propose SCSH, a two-stage stochastic program to staff CRNA shifts. Specifically, SCSH captures the trade-offs between staffing cost, handovers, and under-staffing while accounting

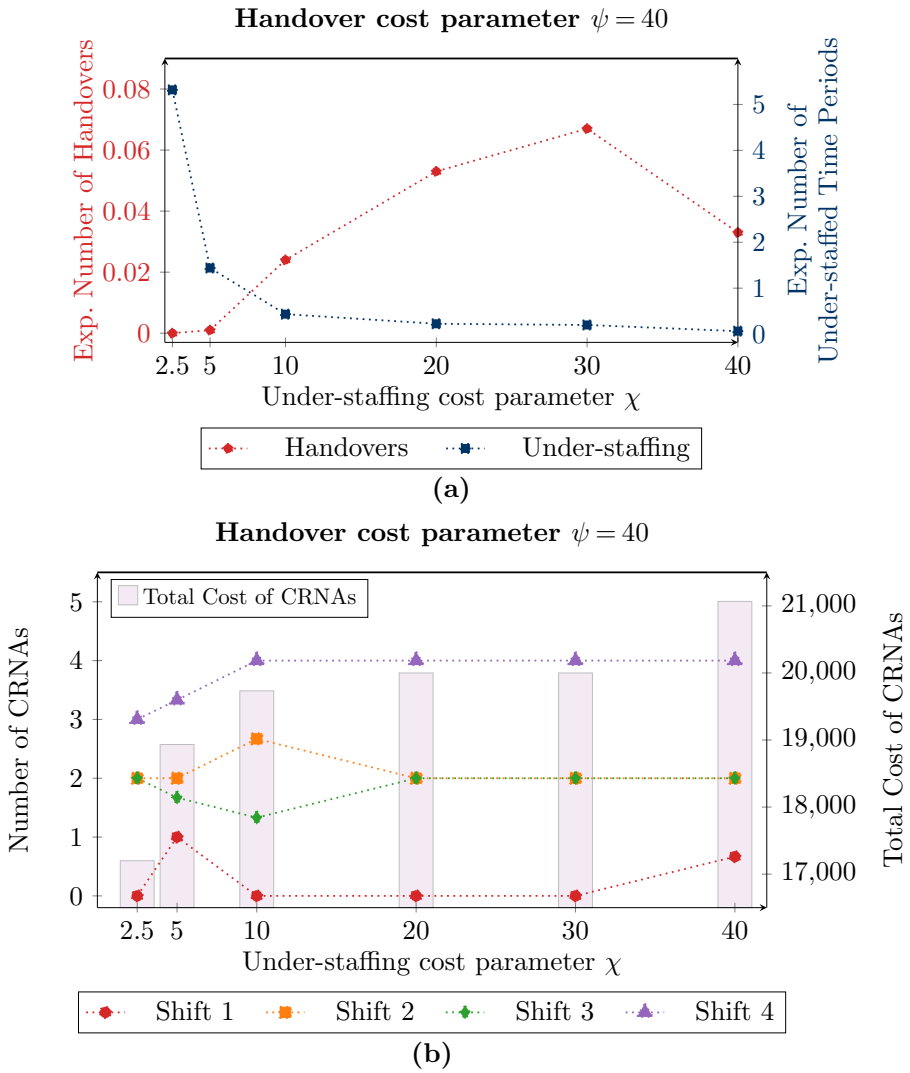

Figure 2 **Analysis of the trade-off between under-staffing and CRNA staffing.**

for uncertainty in surgery durations. Given the daily surgery schedules in ORs, it determines, in the first stage, the number of CRNAs to be called for each shift. In the second stage, on-duty CRNAs are assigned to ORs over the time periods within their shifts. The proposed model captures the trade-offs between CRNA staffing and handover costs under uncertainty in surgery durations. It is broadly applicable to shift-based multi-period scheduling environments in which handovers and under-staffing arise, conditions that are common across many medical institutions and in several other industries. Additionally, our formulation can be extended to incorporate overtime without affecting the proposed solution approach.

We present an Integer L-shaped Algorithm for solving SCSH that incorporates LP Benders Cuts in addition to the standard *no-good* cuts. To further accelerate convergence,

we strengthen these LP Benders Cuts by tightening the second-stage formulation. To this end, we derive valid inequalities for the second-stage problem We demonstrate that the proposed valid inequalities define the convex hull of the nurse assignment and handover constraints. These inequalities are broadly applicable to multi-period scheduling problems that involve preemptive or reactive transfer of tasks across resources. Our computational experiments demonstrate that the proposed valid inequalities are highly effective, leading to substantial improvements in the convergence of the Integer L-shaped Algorithm. They also enhance the performance of the L-shaped Algorithm, enabling it to obtain 0.01-optimal-optimal solutions for a large fraction of the test instances.

This paper demonstrates that explicitly incorporating uncertainty in surgery durations while optimizing the mix of CRNAs across shifts yields meaningful performance improvements over mean-value solutions, without significantly increasing CRNA costs. The resulting stochastic solutions reduce one or both cost components associated with handovers and under-staffing, depending on the trade-offs implied by their relative costs. From an operational perspective, the model reveals how uncertainty compounds over the course of the day, increasing the likelihood of coverage gaps and handovers in later periods. Mitigating these downstream effects may require increasing CRNA hours or opening additional ORs. Overall, the proposed framework provides a principled basis for evaluating and comparing alternative mitigation strategies. These insights and proposed methods are broadly applicable to multi-period scheduling problems involving service transfers across resources. Future research could extend SCSH to jointly optimize both surgery schedules and CRNA assignments. Another promising direction is to incorporate add-on surgeries, which are added to the OR schedule at the last minute, into the modeling framework.

References

Angulo G, Ahmed S, Dey SS (2016) Improving the integer L-shaped method. *INFORMS Journal on Computing* 28(3):483–499.

Bae SH (2021) Relationships between comprehensive characteristics of nurse work schedules and adverse patient outcomes: a systematic literature review. *Journal of Clinical Nursing* 30(15-16):2202–2221.

Bae SH, Fabry D (2014) Assessing the relationships between nurse work hours/overtime and nurse and patient outcomes: systematic literature review. *Nursing Outlook* 62(2):138–156.

Bae SH, Yoon J (2014) Impact of states' nurse work hour regulations on overtime practices and work hours among registered nurses. *Health Services Research* 49(5):1638–1658.

Bansal M, Huang KL, Mehrotra S (2018) Tight second stage formulations in two-stage stochastic mixed integer programs. *SIAM Journal on Optimization* 28(1):788–819.

Birge JR, Louveaux F (2011) *Introduction to Stochastic Programming* (Springer Science & Business Media).

Boet S, Djokhdem H, Leir SA, Théberge I, Mansour F, Etherington C (2020) Association of intraoperative anaesthesia handovers with patient morbidity and mortality: a systematic review and meta-analysis. *British Journal of Anaesthesia* 125(4):605–613.

Breuer DJ, Lahrichi N, Clark DE, Benneyan JC (2020) Robust combined operating room planning and personnel scheduling under uncertainty. *Operations Research for Health Care* 27:100276.

Buddhakulsomsiri J, Kim DS (2006) Properties of multi-mode resource-constrained project scheduling problems with resource vacations and activity splitting. *European Journal of Operational Research* 175(1):279–295.

Conforti M, Cornuéjols G, Zambelli G, Conforti M, Cornuéjols G, Zambelli G (2014) *Integer Programming* (Springer).

Di Martinelly C, Meskens N (2017) A bi-objective integrated approach to building surgical teams and nurse schedule rosters to maximise surgical team affinities and minimise nurses' idle time. *International Journal of Production Economics* 191:323–334.

Gade D, Küçükyavuz S, Sen S (2014) Decomposition algorithms with parametric gomory cuts for two-stage stochastic integer programs. *Mathematical Programming* 144(1):39–64.

Guo M, Wu S, Li B, Rong Y (2014) Maximizing the efficiency of use of nurses under uncertain surgery durations: a case study. *Computers & Industrial Engineering* 78:313–319.

Guo M, Wu S, Li B, Song J, Rong Y (2016) Integrated scheduling of elective surgeries and surgical nurses for operating room suites. *Flexible Services and Manufacturing Journal* 28:166–181.

Hoffman AJ (1976) Total unimodularity and combinatorial theorems. *Linear Algebra and its Applications* 13(1-2):103–108.

Kazemian P, Dong Y, Rohleder TR, Helm JE, Van Oyen MP (2014) An ip-based healthcare provider shift design approach to minimize patient handoffs. *Health Care Management Science* 17:1–14.

Kim K, Mehrotra S (2015) A two-stage stochastic integer programming approach to integrated staffing and scheduling with application to nurse management. *Operations Research* 63(6):1431–1451.

Kirti M, Maurya AK, Yadav RS (2024) Fault-tolerant allocation of deadline-constrained tasks through preemptive migration in heterogeneous cloud environments. *Cluster Computing* 27(8):11427–11454.

Küçükyavuz S, Sen S (2017) An introduction to two-stage stochastic mixed-integer programming. *Leading Developments from INFORMS Communities*, 1–27 (INFORMS).

Kutanoglu E, Sabuncuoglu I (2001) Routing-based reactive scheduling policies for machine failures in dynamic job shops. *International Journal of Production Research* 39(14):3141–3158.

Laporte G, Louveaux FV (1993) The integer l-shaped method for stochastic integer programs with complete recourse. *Operations Research Letters* 13(3):133–142.

Latorre-Núñez G, Lüer-Villagra A, Marianov V, Obreque C, Ramis F, Neriz L (2016) Scheduling operating rooms with consideration of all resources, post anesthesia beds and emergency surgeries. *Computers & Industrial Engineering* 97:248–257.

Lim GJ, Mobasher A, Bard JF, Najjarbashi A (2016) Nurse scheduling with lunch break assignments in operating suites. *Operations Research for Health Care* 10:35–48.

Mobasher A, Lim G, Bard JF, Jordan V (2011) Daily scheduling of nurses in operating suites. *IIE Transactions on Healthcare Systems Engineering* 1(4):232–246.

Neyshabouri S, Berg BP (2017) Two-stage robust optimization approach to elective surgery and downstream capacity planning. *European Journal of Operational Research* 260(1):21–40.

Rath S, Rajaram K, Mahajan A (2017) Integrated anesthesiologist and room scheduling for surgeries: Methodology and application. *Operations Research* 65(6):1460–1478.

Saager L, Hesler BD, You J, Turan A, Mascha EJ, Sessler DI, Kurz A (2014) Intraoperative transitions of anesthesia care and postoperative adverse outcomes. *Anesthesiology* 121(4):695–706.

Salvadori I, Agnetis A (2025) The impact of the number of preemptions in resource-constrained project scheduling problems with time-varying resources: computational experiments and a case study. *Annals of Operations Research* 1–30.

Sen S, Higle JL (2005) The C^3 theorem and a D^2 algorithm for large scale stochastic mixed-integer programming: Set convexification. *Mathematical Programming* 104:1–20.

Smalley HK, Keskinocak P, Vats A (2015) Physician scheduling for continuity: an application in pediatric intensive care. *Interfaces* 45(2):133–148.

Sun K, Sun M, Agrawal D, Dravenstott R, Rosinia F, Roy A (2023) Equitable anesthesiologist scheduling under demand uncertainty using multiobjective programming. *Production and Operations Management* 32(11):3699–3716.

Tsang MY, Shehadeh KS, Curtis FE, Hochman BR, Brentjens TE (2025) Stochastic optimization approaches for an operating room and anesthesiologist scheduling problem. *Operations Research* 73(3):1430–1458.

Xiang W, Yin J, Lim G (2015) A short-term operating room surgery scheduling problem integrating multiple nurses roster constraints. *Artificial Intelligence in Medicine* 63(2):91–106.

Zhang M, Kucukyavuz S (2014) Finitely convergent decomposition algorithms for two-stage stochastic pure integer programs. *SIAM Journal on Optimization* 24(4):1933–1951.

Zhang S, Tang F, Li X, Liu J, Zhang B (2021) A hybrid multi-objective approach for real-time flexible production scheduling and rescheduling under dynamic environment in industry 4.0 context. *Computers & Operations Research* 132:105267.

Online Supplement

Appendix A: Details of the `L-shaped Algorithm`

The `L-shaped Algorithm` to solve `SCSH` involves relaxing the integrality of the second-stage binary variables and solving the resulting relaxation. Let v^l be the optimal objective function value of the relaxed problem where $v^l \leq v^*$. Let $\bar{\mathbf{r}}$ be the first-stage solution obtained at the termination of the `L-shaped Algorithm`, then $v^u = \sum_{s\in S}\sum_{i\in I} c_s^f \bar{r}_i + \sum_{\omega\in\Omega} p_\omega Q(\omega, \bar{\mathbf{r}})$ given an upper bound on v^*. If $\frac{v^u - v^l}{v^u} \leq \epsilon$, then the `L-shaped Algorithm` yields an ϵ-optimal solution.

We implement `L-shaped Algorithm` for `SCSH` on a single `Branch-and-Bound` tree. We initialize the algorithm by solving the following master problem using the `Branch-and-Bound` algorithm:

$$(\mathcal{M}^L) \quad \text{Min} \quad \sum_{s\in S}\sum_{i\in I} c_s^f r_i + \sum_{\omega\in\Omega} p_\omega \theta_\omega \tag{11a}$$

$$\text{s.t.} \quad r_{i_1} \geq r_{i_2} \qquad \forall s \in S,\ \ i_1, i_2 \in I_s :\ \ i_1 < i_2 \tag{11b}$$

$$\theta_\omega \geq 0 \qquad \forall \omega \in \Omega, \tag{11c}$$

$$\mathbf{r} \in \mathbb{B}^{|I|}. \tag{11d}$$

For each integer feasible solution $(\bar{\mathbf{r}}, \bar{\boldsymbol{\theta}})$ encountered within any node of the `Branch-and-Bound` tree, we solve the following subproblem for each scenario $\omega \in \Omega$:

$$Q^l(\omega, \bar{\mathbf{r}}^k) = \text{Min} \ \sum_{i\in I}\sum_{t\in T} c^h w_{it}(\omega) + \sum_{j\in J}\sum_{t\in T} c^i x_{i_d jt}(\omega) + \sum_{i\in I}\sum_{t\in T} c^h \bar{w}_{it}(\omega) \tag{12a}$$

$$\text{s.t.} \ (\mu^1_{ijt}) \quad w_{it}(\omega) \geq x_{ijt}(\omega) - x_{ij(t+1)}(\omega) \qquad \forall i \in I, j \in J_t(\omega), t \in T \setminus \{|T|\}, \tag{12b}$$

$$(\mu^2_{ijt}) \quad \bar{w}_{it}(\omega) \geq x_{i_d jt}(\omega) + x_{ij(t+1)}(\omega) - 1 \qquad \forall i \in I, j \in J_t(\omega), t \in T \setminus \{|T|\}, \tag{12c}$$

$$(\mu^3_{ist}) \quad \sum_{j\in J} x_{ijt}(\omega) \leq \bar{r}_i^t z_{st} \qquad \forall i \in I, s \in S, t \in T, \tag{12d}$$

$$(\mu^4_{jt}) \quad \sum_{i\in I} x_{ijt}(\omega) + x_{i_d jt}(\omega) = \alpha_{jt}(\omega) \qquad \forall j \in J, t \in T, \tag{12e}$$

$$(\mu^5_{it}) \quad w_{it}(\omega) \leq 1 \qquad \forall i \in I, t \in T \setminus \{|T|\}, \tag{12f}$$

$$(\mu^6_{it}) \quad \bar{w}_{it}(\omega) \leq 1 \qquad \forall i \in I, t \in T \setminus \{|T|\}, \tag{12g}$$

$$(\mu^7_{ijt}) \quad x_{ijt}(\omega) \leq 1 \qquad \forall i \in I, j \in J, t \in T, \tag{12h}$$

$$\mathbf{w}(\omega), \bar{\mathbf{w}}(\omega), \mathbf{x}(\omega) \geq 0 \tag{12i}$$

The notation for the optimal dual solution is stated in parentheses before the constraints. For each $\omega \in \Omega$, if $Q^l(\omega, \bar{\mathbf{r}}^k) > \bar{\theta}^k(\omega)$, the following optimality cut is added to $\mathcal{M}^L$ to exclude the solution $(\bar{\mathbf{r}}, \bar{\boldsymbol{\theta}})$:

$$\begin{aligned}\theta_\omega \geq & - \sum_{\substack{i\in I, j\in J_t(\omega),\\ t\in T\setminus\{|T|\}}} \mu^2_{ijt} + \sum_{\substack{i\in I,\\ s\in S, t\in T}} \mu^3_{ist} r_i z_{st} + \sum_{j\in J, t\in T} \mu^4_{jt}\alpha_{jt}(\omega) \\ & + \sum_{i\in I, t\in T\setminus\{|T|\}} \mu^5_{it} + \sum_{i\in I, t\in T\setminus\{|T|\}} \mu^6_{it} + \sum_{i\in J, j\in J, t\in T} \mu^7_{ijt}.\end{aligned} \tag{13}$$

Appendix B: Proof of Propositions

Proof of Proposition 1: Assume that for some $(\mathbf{x}^*, \mathbf{w}^*, \bar{\mathbf{w}}^*) \in \mathcal{P}(\mathbf{r})$, there exists an $i \in I$, $t \in T \setminus \{|T|\}$, and $\bar{J} \subseteq J_t$ such that:

$$w^*_{it} < \sum_{j\in\bar{J}} \left(x^*_{ijt} - x^*_{ij(t+1)}\right) \tag{14}$$

Then, from (2b) and (2f), it must be that $w^*_{it} = 0$ and $\exists j_1 \in \bar{J}$ such that $x^*_{ij_1t} = 1, x^*_{ij_1(t+1)} = 0$. In that case, however, (2c) enforces $w^*_{it} \geq 1$, which is a contradiction. $\square$

Proof of Proposition 2: For the ease of presentation, we use x_{j1} to represent x_{ijt}, x_{j2} in place of $x_{ij(t+1)}$, and w for w_{it}. We represent $\mathcal{Q}_{it}$ as the union of two disjoint sets as $P_1 \cup P_2$, where

$$P_1 = \begin{cases} x_{j1} - x_{j2} - w \leq 0, & \forall j \in J_t, \\ \sum_{j\in J_t} x_{j1} \leq 1, & \\ \sum_{j\in J_t} x_{j2} \leq 1, & \\ x_{j1}, x_{j2} \in \{0,1\} & \forall j \in J_t, \\ w = 1. & \end{cases} \qquad P_2 = \begin{cases} x_{j1} - x_{j2} - w \leq 0, & \forall j \in J_t, \\ \sum_{j\in J_t} x_{j1} \leq 1, & \\ \sum_{j\in J_t} x_{j2} \leq 1, & \\ x_{j1}, x_{j2} \in \{0,1\} & \forall j \in J_t, \\ w = 0. & \end{cases}$$

Let $\tilde{P}_1$ and $\tilde{P}_2$ be the linear programming relaxations of P_1 and P_2, respectively. As the constraint matrices for the variables $x_{j1}, x_{j2}\ \forall j \in J_t$ are totally unimodular (TU), $\text{conv}(P_1) = \tilde{P}_1$ and $\text{conv}(P_2) = \tilde{P}_1$. Consequently, as $\tilde{P}_1$ and $\tilde{P}_2$ are bounded, $\text{conv}(\mathcal{Q}_{it}) = \text{conv}(\tilde{P}_1 \cup \tilde{P}_2)$ (Conforti et al. 2014). Furthermore, $\text{conv}(\tilde{P}_1 \cup \tilde{P}_2)$ is given by the projection of the following polyhedron onto the $(\mathbf{x_1}, \mathbf{x_2}, w)$ variable space (Conforti et al. 2014).

$$x^1_{j1} - x^1_{j2} - w^1 \leq 0, \qquad x^2_{j1} - x^2_{j2} - w^2 \leq 0, \qquad \forall j \in J_t, \tag{15a}$$

$$\sum_{j\in J_t} x^1_{j1} \le \lambda^1, \qquad \sum_{j\in J_t} x^2_{j1} \le \lambda^2, \tag{15b}$$

$$\sum_{j\in J_t} x^1_{j2} \le \lambda^1, \qquad \sum_{j\in J_t} x^2_{j2} \le \lambda^2, \tag{15c}$$

$$w^1 = \lambda^1, \qquad w^2 = 0, \tag{15d}$$

$$x^1_{j1}, x^1_{j2} \ge 0, \qquad x^2_{j1}, x^2_{j2} \ge 0, \qquad \forall j \in J_t, \tag{15e}$$

$$x^1_{j1} + x^2_{j1} = x_{j1}, \qquad \forall j \in J_t, \tag{15f}$$

$$x^1_{j2} + x^2_{j2} = x_{j2}, \qquad \forall j \in J_t, \tag{15g}$$

$$w^1 + w^2 = w, \tag{15h}$$

$$\lambda^1 + \lambda^2 = 1, \tag{15i}$$

$$0 \le \lambda^1, \lambda^2 \le 1. \tag{15j}$$

From (15d), (15f), (15g), (15h) and (15i), we get the equalities $w^1 = w$, $w^2 = 0$, $\lambda^1 = w$, $\lambda^2 = (1-w)$, $x^2_{j1} = x_{j1} - x^1_{j1}$, and $x^2_{j2} = x_{j2} - x^1_{j2}$. Substituting these equalities in the inequalities of (15) we obtain:

$$x_{j1} - x_{j2} \le x^1_{j1} - x^1_{j2} \le w \qquad \forall j \in J_t, \tag{16a}$$

$$-1 + w + \sum_{j\in J_t} x_{j1} \le \sum_{j\in J_t} x^1_{j1} \le w, \tag{16b}$$

$$-1 + w + \sum_{j\in J_t} x_{j2} \le \sum_{j\in J_t} x^1_{j2} \le w, \tag{16c}$$

$$0 \le x^1_{j1} \le x_{j1} \qquad \forall j \in J_t, \tag{16d}$$

$$0 \le x^1_{j2} \le x_{j2} \qquad \forall j \in J_t. \tag{16e}$$

Substituting $x_{j1} = x_{ijt}$, $x_{j2} = x_{ij(t+1)}$, and $w = w_{it}$ in (16), we get $\mathcal{V}_{it}$. □

Next, we state the *Hoffman's Circulation Theorem* (Hoffman 1976), which is a key component required for the proof of Proposition 3. l

LEMMA 1. *Hoffman Circulation Theorem (1976): Let $G = (V, E)$ be a directed graph. Let $\ell, u : E \mapsto \mathbb{R} \cup \{\pm\infty\}$ denote the lower and upper bounds of flow on arc e. Assume that $\ell(e) \le u(e)$ for every $e \in E$. Then, there exists a feasible flow $\sigma : E \mapsto \mathbb{R}$ that satisfies (i) $\ell(e) \le \sigma(e) \le u(e)$ for every $e \in E$, and (ii) $\sum_{(a,b)\in E} \sigma(a,b) = \sum_{(b,a)\in E} \sigma(b,a)$ for all $a \in V$, if and only if*

$$\sum_{(a,b)\in\delta^+(X)} \ell(a,b) \le \sum_{(a,b)\in\delta^-(X)} u(a,b) \qquad \forall X \subseteq V \tag{17}$$

where $\delta^-(X) := \{(a,b) \in E : a \notin X, b \in X\}$ *and* $\delta^+(X) := \{(a,b) \in E : a \in X, b \notin X\}$.

A feasible flow σ that satisfies conditions (i) and (ii) specified in Lemma 1 is referred to as a *circulation*.

Proof of Proposition 3: For the ease of presentation, we use x_{j1} to represent x_{ijt}, x_{j2} in place of $x_{ij(t+1)}$, and w for w_{it}. Consider the directed graph $G(\bar{V}, \bar{E})$ shown in Figure 3 with $\sigma(a,b)$ representing the flow along the arc $(a,b) \in \bar{E}$, and $\ell(a,b)$ and $u(a,b)$ denote the lower and upper bounds, respectively, for $\sigma(a,b)$. In $G(\bar{V}, \bar{E})$, $\bar{V} = \{d_1, d_2, q\} \cup \{p_j, j \in J_t\}$, $\bar{E} = \{(d_1, p_j), \forall j \in J_t\} \cup \{(p_j, q), \forall j \in J_t\} \cup \{(p_j, d_2), \forall j \in J_t\} \cup \{(q, d_2), (d_2, d_1)\}$. Denote $\sigma(d_1, p_j)$ by x^1_{j1} $\forall j \in J_t$, $\sigma(p_j, q)$ by x^1_{j2} $\forall j \in J_t$, and let

$$\ell(a,b) = \begin{cases} 0 & a = d_1, b = p_j \ \ \forall j \in J_t \\ x_{j1} - x_{j2} & a = p_j, b = d_2 \ \ \forall j \in J_t \\ 0 & a = p_j, b = q \ \ \forall j \in J_t \\ -1 + w + \sum_{j \in J_t} x_{j2} & a = q, b = d_2 \\ -1 + w + \sum_{j \in J_t} x_{j1} & a = d_2, b = d_1 \end{cases} \qquad u(a,b) = \begin{cases} x_{j1} & a = d_1, b = p_j \ \ \forall j \in J_t \\ w & a = p_j, b = d_2 \ \ \forall j \in J_t \\ x_{j2} & a = p_j, b = q \ \ \forall j \in J_t \\ w & a = q, b = d_2 \\ w & a = d_2, b = d_1 \end{cases}$$

Applying the two conditions in Lemma 1 to $G(\bar{V}, \bar{E})$, we obtain:

$$0 \le \sigma(d_1, p_j) = x^1_{j1} \le x_{j1} \qquad \forall j \in J_t \tag{18a}$$

$$x_{j1} - x_{j2} \le \sigma(p_j, d_2) \le w \qquad \forall j \in J_t \tag{18b}$$

$$0 \le \sigma(p_j, q) = x^1_{j2} \le x_{j2} \qquad \forall j \in J_t \tag{18c}$$

$$-1 + w + \sum_{j \in J_t} x_{j2} \le \sigma(q, d_2) \le w \tag{18d}$$

$$-1 + w + \sum_{j \in J_t} x_{j1} \le \sigma(d_2, d_1) \le w \tag{18e}$$

$$\sigma(p_j, d_2) = x^1_{j1} - x^1_{j2} \qquad \forall j \in J_t \tag{18f}$$

$$\sigma(q, d_2) = \sum_{j \in J_t} x^1_{j2} \tag{18g}$$

$$\sigma(d_2, d_1) = \sum_{j \in J_t} x^1_{j1} \tag{18h}$$

In particular, (18a)-(18e) and (18f)-(18h) are obtained by applying (i) and (ii), respec-

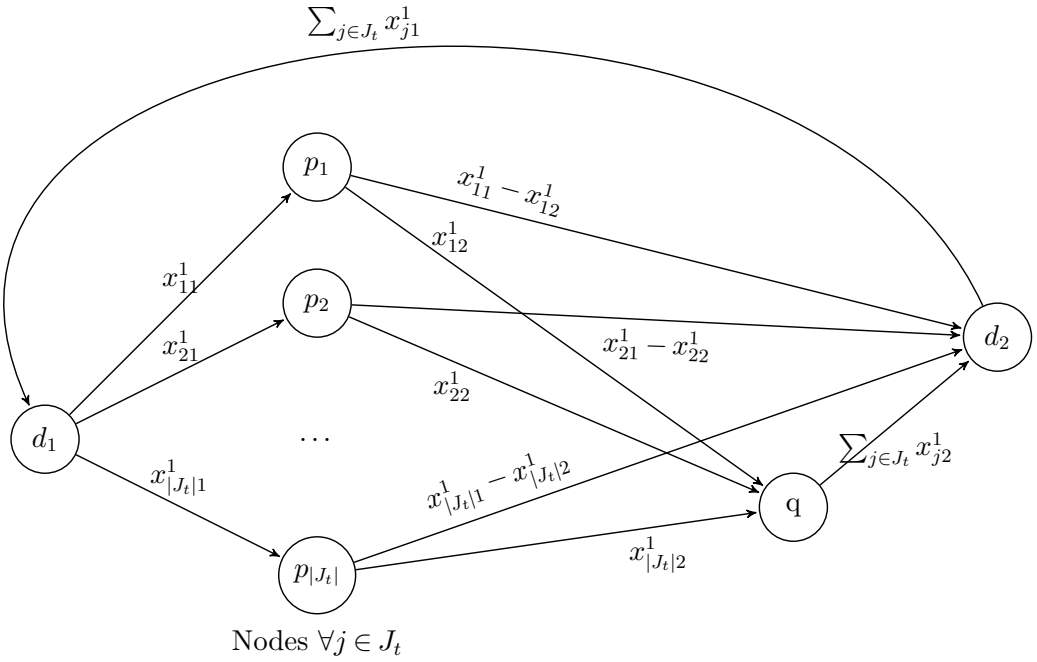

Figure 3 $G(\bar{V}, \bar{E})$ **for the Proof of Proposition 3. The labels on the arcs indicate the flow variables.**

tively. Using the equalities in (18f), (18g) and (18h) in (18b), (18d) and (18e), respectively, we get the constraint set (16) that define $\mathcal{V}_{it}$. Thus, a circulation exists on $G(\bar{V}, \bar{E})$ if and only if $\mathcal{V}_{it} \neq \emptyset$.

Next, we apply (17) to $G(\bar{V}, \bar{E})$ to derive another condition for the existence of a circulation. Let $\bar{J} \subseteq \{p_j : j \in J_t\}$. Note that $\bar{J}$ can be empty. Consider the following cases:

Case 1. $X = \{d_1, [p_j]_{j\in\bar{J}}\}$: For this case, $\delta^+(X) = \{\{(p_j, q) \ \forall j \in \bar{J}\} \cup \{(p_j, d_2) \ \forall j \in \bar{J}\} \cup \{(d_1, p_j) \ \forall j \in J_t \setminus \bar{J}\}$, $\delta^-(X) = \{(d_2, d_1)\}$. (17) $\Rightarrow$

$$\sum_{j\in\bar{J}} \ell(p_j, q) + \sum_{j\in\bar{J}} \ell(p_j, d_2) + \sum_{j\in J\setminus\bar{J}} \ell(d_1, p_j) \leq u(d_2, d_1)$$
$$\Rightarrow \sum_{j\in\bar{J}} (x_{j1} - x_{j2}) \leq w \tag{19}$$

Case 2. $X = \{[p_j]_{j\in\bar{J}}\}$: For this case, $\delta^+(X) = \{(p_j, q) \ \forall j \in \bar{J}\} \cup \{(p_j, d_2) \ \forall j \in \bar{J}\}$, $\delta^-(X) = \{(d_1, p_j) \ \forall j \in \bar{J}\}$. (17) $\Rightarrow$

$$\sum_{j\in\bar{J}} \ell(p_j, q) + \sum_{j\in\bar{J}} \ell(p_j, d_2) \leq \sum_{j\in\bar{J}} u(d_1, p_j)$$

$$\Rightarrow \sum_{j\in\bar{J}}(x_{j1}-x_{j2}) \leq \sum_{j\in\bar{J}} x_{j1}$$
$$\Rightarrow \sum_{j\in\bar{J}} x_{j2} \geq 0 \tag{20}$$

Case 3. $X = \{[p_j]_{j\in\bar{J}}, q\}$: For this case, $\delta^+(X) = \{(p_j, d_2)\ \forall j \in \bar{J}\} \cup (q, d_2)$, $\delta^-(X) = \{(d_1, p_j)\ \forall j \in \bar{J}\} \cup \{(p_j, q)\ \forall j \in J_t \setminus \bar{J}\}$. (17) $\Rightarrow$

$$\sum_{j\in\bar{J}} \ell(p_j, d_2) + \ell(q, d_2) \leq \sum_{j\in\bar{J}} u(d_1, p_j) + \sum_{J_t\setminus\bar{J}} u(p_j, q)$$
$$\Rightarrow \sum_{j\in\bar{J}}(x_{j1}-x_{j2}) - 1 + w + \sum_{j\in J_t} x_{j2} \leq \sum_{j\in\bar{J}} x_{j1} + \sum_{J_t\setminus\bar{J}} x_{j2}$$
$$\Rightarrow w \leq 1 \tag{21}$$

Case 4. $X = \{[p_j]_{j\in\bar{J}}, d_2\}$: For this case, $\delta^+(X) = \{(p_j, q)\ \forall j \in \bar{J}\} \cup (d_2, d_1)$, $\delta^-(X) = \{(d_1, p_j)\ \forall j \in \bar{J}\} \cup \{(p_j, d_2)\ \forall j \in J_t \setminus \bar{J}\} \cup (q, d_2)$. (17) $\Rightarrow$

$$\sum_{j\in\bar{J}} \ell(p_j, q) + \ell(d_2, d_1) \leq \sum_{j\in\bar{J}} u(d_1, p_j) + \sum_{j\in J_t\setminus\bar{J}} u(p_j, d_2) + u(q, d_2)$$
$$\Rightarrow -1 + w + \sum_{j\in J_t} x_{j1} \leq \sum_{j\in\bar{J}} x_{j1} + \sum_{j\in J_t\setminus\bar{J}} w + w$$
$$\Rightarrow \sum_{j\in J_t\setminus\bar{J}} x_{j1} \leq |J_t \setminus \bar{J}|w + 1 \tag{22}$$

Case 5. $X = \{d_1, [p_j]_{j\in\bar{J}}, d_2\}$: For this case, $\delta^+(X) = \{(p_j, q)\ \forall j \in \bar{J}\} \cup \{(d_1, p_j)\ \forall j \in J_t \setminus \bar{J}\}$, $\delta^-(X) = \{(p_j, d_2)\ \forall j \in J_t \setminus \bar{J}\} \cup (q, d_2)$. (17) $\Rightarrow$

$$\sum_{j\in\bar{J}} \ell(p_j, q) + \sum_{j\in J_t\setminus\bar{J}} \ell(d_1, p_j) \leq \sum_{j\in J_t\setminus\bar{J}} u(p_j, d_2) + u(q, d_2)$$
$$\Rightarrow 0 \leq \sum_{j\in J_t\setminus\bar{J}} w + w$$
$$\Rightarrow w \geq 0 \tag{23}$$

Case 6. $X = \{[p_j]_{j\in\bar{J}}, q, d_2\}$: For this case, $\delta^+(X) = (d_2, d_1)$, $\delta^-(X) = \{(p_j, d_2)\ \forall j \in J_t \setminus \bar{J}\} \cup \{(p_j, q)\ \forall j \in J_t \setminus \bar{J}\} \cup \{(d_1, p_j)\ \forall j \in \bar{J}\}$. (17) $\Rightarrow$

$$\ell(d_2, d_1) \leq \sum_{j\in J_t\setminus\bar{J}} u(p_j, d_2) + \sum_{j\in J_t\setminus\bar{J}} u(p_j, q) + \sum_{j\in\bar{J}} u(d_1, p_j)$$

$$\Rightarrow -1 + w + \sum_{j\in J_t} x_{j1} \le \sum_{j\in J_t\setminus\bar{J}} w + \sum_{j\in J_t\setminus\bar{J}} x_{j2} + \sum_{j\in\bar{J}} x_{j1}$$
$$\Rightarrow \sum_{j\in J_t\setminus\bar{J}} (x_{j1} - x_{j2}) \le (|J_t\setminus\bar{J}|-1)w + 1 \tag{24}$$

Case 7. $X = \{d_1, [p_j]_{j\in\bar{J}}, q\}$: For this case, $\delta^+(X) = \{(p_j, d_2)\ \ \forall j \in \bar{J}\} \cup \{(d_1, p_j)\ \ \forall j \in J_t\setminus\bar{J}\} \cup (q, d_2)$, $\delta^-(X) = (d_2, d_1) \cup \{(p_j, q)\ \ \forall j \in J_t\setminus\bar{J}\}$. (17) $\Rightarrow$

$$\sum_{j\in\bar{J}} \ell(p_j, d_2) + \sum_{j\in J_t\setminus\bar{J}} \ell(d_1, p_j) + \ell(q, d_2) \le \sum_{j\in J_t\setminus\bar{J}} u(p_j, q) + u(d_2, d_1)$$
$$\Rightarrow \sum_{j\in\bar{J}} (x_{j1} - x_{j2}) - 1 + w + \sum_{j\in J_t} x_{j2} \le \sum_{j\in J_t\setminus\bar{J}} x_{j2} + w$$
$$\Rightarrow \sum_{j\in\bar{J}} x_{j1} \le 1 \tag{25}$$

Case 8. $X = \{d_1, [p_j]_{j\in\bar{J}}, q, d_2\}$: For this case, $\delta^+(X) = \{(d_1, p_j)\ \ \forall j \in J_t\setminus\bar{J}\}$, $\delta^-(X) = \{(p_j, q)\ \ \forall j \in J_t\setminus\bar{J}\} \cup \{(p_j, d_2)\ \ \forall j \in J_t\setminus\bar{J}\}$. (17) $\Rightarrow$

$$\sum_{j\in J_t\setminus\bar{J}} \ell(d_1, p_j) \le \sum_{j\in J_t\setminus\bar{J}} u(p_j, q) + \sum_{j\in J_t\setminus\bar{J}} u(p_j, d_2)$$
$$\Rightarrow \sum_{j\in J_t\setminus\bar{J}} x_{j2} + \sum_{j\in J_t\setminus\bar{J}} w \ge 0 \tag{26}$$

Cases 1-8 cover all possible $X \subseteq \bar{V}$ since $\bar{J}$ can be empty. Non-dominated constraints among (19)-(26) are:

$$\sum_{j\in\bar{J}} (x_{j1} - x_{j2}) \le w \qquad \forall \bar{J} \subseteq J_t, \tag{27a}$$
$$\sum_{j\in J_t} x_{j1} \le 1,\ 0 \le w \le 1,\ x_{j2} \ge 0. \tag{27b}$$

By definition, $\ell(a, b) \le u(a, b)\ \ \forall (a, b) \in \bar{E}$. From this condition, we obtain:

$$\sum_{j\in J_t} x_{j1} \le 1,\ \sum_{j\in J_t} x_{j2} \le 1, \tag{28a}$$
$$x_{j1} \ge 0,\ x_{j2} \ge 0 \qquad \forall j \in J_t. \tag{28b}$$

From Lemma 1, there exists a circulation on $G(\bar{V}, \bar{E})$ if and only if (27)-(28) are feasible. Therefore, $\mathcal{V}_{it} \ne \emptyset$ if and only if both (27) and (28) are feasible. Combining (27)-(28) and substituting $x_{j1} = x_{ijt}$, $x_{j2} = x_{ij(t+1)}$, and $w = w_{it}$, we obtain

$$\sum_{j\in\bar{J}} (x_{ijt} - x_{ij(t+1)}) \le w_{it} \qquad \forall \bar{J} \subseteq J_t, \tag{29a}$$

$$\sum_{j\in J_t} x_{ijt} \le 1,\ \sum_{j\in J_t} x_{ij(t+1)} \le 1, \tag{29b}$$

$$x_{ijt} \ge 0,\ x_{ij(t+1)} \ge 0,\ 0 \le w_{it} \le 1 \tag{29c}$$

which coincides exactly with the constraint set defining $\tilde{\mathcal{Q}}^L_{it}$. Thus, for every $(w_{it}, \mathbf{x}_{it}, \mathbf{x}_{i(t+1)}) \in \tilde{\mathcal{Q}}^L_{it}$, as $\mathcal{V}_{it} \neq \emptyset$, $\exists(\mathbf{x}^1_{it}, \mathbf{x}^2_{i(t+1)})$ such that $(w_{it}, \mathbf{x}_{it}, \mathbf{x}_{i(t+1)}, \mathbf{x}^1_{it}, \mathbf{x}^2_{i(t+1)}) \in \mathcal{V}_{it}$. As a result, $\tilde{\mathcal{Q}}^L_{it} = \text{Proj}_{(w_{it}, \mathbf{x}_{it}, \mathbf{x}_{i(t+1)})}\, \mathcal{V}_{it}$. $\square$

Proof of Proposition 4: For some $i \in I$, $t \in T \setminus \{|T|\}$, consider the inequalities (5):

$$w_{it} \ge \sum_{j\in\bar{J}} \left(x_{ijt} - x_{ij(t+1)}\right) \qquad \forall \bar{J} \subseteq J_t \tag{30a}$$

$$\Rightarrow w_{it} \ge \max_{\bar{J}\subseteq J_t} \sum_{j\in\bar{J}} \left(x_{ijt} - x_{ij(t+1)}\right) \tag{30b}$$

$$\Rightarrow w_{it} \ge \eta_{it} = \max \sum_{j\in J_t} \left(x_{ijt} - x_{ij(t+1)}\right) y_j \tag{30c}$$

$$\text{s.t. } 0 \le y_j \le 1 \qquad \forall j \in J_t. \tag{30d}$$

Here, $y_j \ge 0$ due to $w_{it} \ge 0$. Dualizing the LP defining η_{it} we get:

$$\eta_{it} = \min \sum_{j\in J_t} \beta_{ijt} \tag{31a}$$

$$\text{s.t. } \beta_{ijt} \ge x_{ijt} - x_{ij(t+1)} \qquad \forall j \in J_t, \tag{31b}$$

$$\beta_{ijt} \ge 0 \qquad \forall j \in J_t. \tag{31c}$$

Combining (30c), (30d) and (31), we get (9). $\square$

Proof of Proposition 5: Assume that for some $(\mathbf{x}^*, \mathbf{w}^*, \bar{\mathbf{w}}^*) \in \mathcal{P}(\mathbf{r})$, there exists an $i \in I$, $t \in T \setminus \{|T|\}$, and $j' \in J$ such that:

$$w^*_{it} < x^*_{ij'(t+1)} - 1 + \sum_{j\in J_t\setminus j'} x^*_{ijt} \tag{32}$$

Following (2b), (2f) and (32), $w^*_{it} = 0$ and $x^*_{ij'(t+1)} + \sum_{j\in J_t\setminus j'} x^*_{ijt} = 2$. This implies, due to (2b), that $x^*_{ij'(t+1)} = 1$ and $\exists j_2 \in J_t \setminus j'$ such that $x^*_{ij_2t} = 1$. From (2c) for i, j_2, t, it follows that $w^*_{it} \ge 1$, which is a contradiction. $\square$

Proof of Proposition 6: For some $i \in I$, $t \in T \setminus \{|T|\}$ and $j' \in J$ valid inequality (5) for i, t and $\bar{J} = J_t \setminus j'$ is stated as:

$$w_{it} \ge \sum_{j\in J_t\setminus j'} x_{ijt} - \sum_{j\in J_t\setminus j'} x_{ij(t+1)} \ge x_{ij'(t+1)} - 1 + \sum_{j\in J_t\setminus j'} x_{ijt}$$

where the last inequality is due to (2b). $\square$

Appendix C: Surgery Data

Table 10 Summary of 353-Day surgery data

Specialty	Duration average (min)	Duration standard deviation (min)	Case mix (%)
Dentistry	131	39	1.77
Gastroenterology	71	47	0.28
General	67	39	1.16
Gynecology	87	53	5.22
Gynecology Oncology	52	0	0.01
Interventional Radiology	52	4	0.01
Neurology	44	8	0.14
Obstetrics	53	17	0.01
Ophthalmology	47	32	23.42
Oral Surgery	100	46	0.05
Orthopedics	98	51	14.59
Otolaryngology	109	77	13.05
Pain	61	35	1.53
Pediatric Gastroenterology	50	1	0.01
Pediatric General	93	30	0.05
Pediatric Ophthalmology	65	25	3.82
Pediatric Orthopedics	94	35	0.17
Pediatric Urology	60	33	1.06
Plastics	88	58	1.84
Podiatry	104	69	1.48
Pediatric ENT	72	58	3.95
Pediatric Neurology	42	25	0.07
Surgical Oncology	99	56	2.90
Urology	51	34	23.40

Table 11 Surgery Scheduling Details - Day 1

Specialty		(OR, starting time period)
Type	No of Surgeries	
Ophthalmology	20	(7, 1), (4, 1), (4, 3), (7, 4), (7, 7), (4, 8), (4, 9), (7, 10), (7, 13), (7, 16), (7, 19), (4, 21), (7, 22), (7, 25), (4, 27), (7, 28), (4, 30), (7, 31), (4, 33), (7, 34)
Orthopedics	11	(5, 1),(2, 1), (6, 1), (2, 4), (5, 8), (2, 8), (2, 14), (2, 17), (5, 19), (5, 26), (5, 32)
Otolaryngology	4	(3, 1), (3, 4), (1, 11), (3, 15)
Pediatric ENT	6	(1, 1), (1, 4), (1, 6), (1, 21), (1, 27), (1, 33)
Urology	15	(9, 2), (9, 6), (8, 7), (9, 11), (8, 11), (8, 14), (9, 15), (8, 16), (8, 18), (9, 19), (8, 24), (9, 27), (8, 29), (9, 33), (9, 39)

Table 12 Surgery Scheduling Details - Day 2

Specialty		(OR, starting time period)
Type	No of Surgeries	
Gynecology	7	(2, 1), (2, 10), (2, 16), (2, 20), (2, 24), (2, 28), (2, 33)
Ophthalmology	9	(7, 5), (7, 7), (7, 11), (7, 16), (7, 20), (7, 23), (7, 27), (5, 28), (7,31)
Oral Surgery	1	(3, 33)
Orthopedics	9	(6, 1), (4, 1), (5, 1), (4, 10), (6, 12), (5, 18), (4, 19), (6, 25), (6, 31)
Otolaryngology	2	(3, 1), (3, 14)
Pediatric Urology	3	(8, 6), (8, 12), (8, 18)
Pediatric ENT	3	(1, 1), (1, 16), (1, 24)
Urology	7	(9, 1), (9, 7), (9, 13), (9, 19), (9, 25), (9, 31), (9, 35)

Table 13 Surgery Scheduling Details - Day 3

Specialty		(OR, starting time period)
Type	No of Surgeries	
Ophthalmology	12	(7, 1), (4, 1), (7, 3), (7, 6), (4, 8), (7, 9), (7, 12), (4, 14), (7, 15), (4, 20), (4, 26), (4, 31)
Orthopedics	7	(5, 1), (6, 1), (6, 4), (6, 9), (6, 14), (5, 21), (1, 33)
Otolaryngology	4	(3, 1), (1, 1), (3, 9), (1, 12)
Pediatric Ophthalmology	3	(7, 18),(7, 24), (7, 29)
Surgical Oncology	5	(2, 1), (2, 8), (2, 16), (2, 23), (2, 31)
Urology	6	(9, 9), (6, 23), (9, 25), (8, 27), (6, 30), (9, 3)

Appendix D: $SS_{\mathbf{r},\omega}$ with overtime

Let c^o be the per-period cost of CRNA overtime and $T_i = \{1, 2, 3, \ldots, |T_i|\}$ be the set of time periods covered by the shift of CRNA i. Let $\zeta_{it}(\omega)$ be a binary variable that equals 1 if time period t is the last period after the shift end in which CRNA i is assigned to an OR under scenario ω, and 0 otherwise. Using these notations, $SS_{\mathbf{r},\omega}$ with CRNA overtime is given by:

$$\text{Min} \sum_{i\in I}\sum_{t\in T} c^h w_{it}(\omega) + \sum_{i\in I}\sum_{t\in T} c^h \bar{w}_{it}(\omega) + \sum_{j\in J}\sum_{t\in T} c^i x_{i_d jt}(\omega) + \sum_{i\in I}\sum_{j\in J}\sum_{t\in T\setminus T_i} (t - |T_i|) c^o \zeta_{it}(\omega) \tag{33a}$$

s.t. (2c), (2d), (2e)

$$\sum_{j\in J} x_{ijt}(\omega) \le r_i \qquad \forall i \in I, t \in T, \tag{33b}$$

$$\sum_{\tau=t}^{|T|} \zeta_{i\tau}(\omega) \ge x_{ijt}(\omega) \qquad \forall i \in I, j \in J, t \in T \setminus T_i\,, \tag{33c}$$

$$\boldsymbol{\zeta}(\omega) \in \mathbb{B}^{(|I|)\times|T\setminus T_i|}\,, \tag{33d}$$

$$\mathbf{x}(\omega) \in \mathbb{B}^{(|I|+1)\times|J|\times|T|},\ \ \mathbf{w}(\omega), \bar{\mathbf{w}}(\omega) \in \mathbb{B}^{(|I|)\times(|T|-1)}\,. \tag{33e}$$

(33b) ensures that CRNAs are allocated to ORs only if they are called while (33c) tracks the last time period in which CRNAs are allocated to an OR after their shift ends. Lastly, the first three terms of the objective function (33a) are same as (2a) while the last term models the total overtime cost.

Appendix E: Comparison of Stochastic Solution and Mean Value Solution for $|\Omega| = 1000$

Table 14 Comparison of Stochastic Solution and Mean Value Solution for $|\Omega| = 1000$.

Case	ψ—χ	VSS	κ_{HO}	κ_{US}	κ_{SC}	κ_{S_1}	κ_{S_2}	κ_{S_3}	κ_{S_4}
1	30—5	2.90	-11.58	10.17	-2.33	44.44	-40.00	0.00	0.00
2	30—10	5.12	4.10	10.43	-2.33	44.44	-40.00	0.00	0.00
3	30—20	5.56	10.82	8.90	-5.26	33.33	-62.22	0.00	0.00
4	40—5	2.58	-12.36	8.01	-2.07	38.89	-34.44	0.00	0.00
5	40—10	4.98	-1.72	10.82	-2.33	44.44	-40.00	0.00	0.00
6	40—20	6.59	9.64	9.25	-2.54	55.56	-51.11	0.00	0.00
7	50—5	2.51	-9.90	7.34	-2.07	38.89	-34.44	0.00	0.00
8	50—10	4.75	-5.90	10.48	-2.33	44.44	-40.00	0.00	0.00
9	50—20	6.61	6.80	10.34	-3.57	50.00	-51.11	0.00	0.00